1. Title

Temozolomide-fatty acid conjugates for glioblastoma multiforme: in vitro and in vivo evaluation.

2. Introduction

Glioblastoma multiforme (GBM) is the most challenging brain tumor that occurs in primary astrocytes and accounts for 60% of all primary brain tumors in adults [1]. Despite the availability of chemotherapies for the treatment of GBM, the median survival rate for glioma tumor patients is <14 months [2]. WHO classified brain tumors into four major grades, namely I to IV, based on the severity and histopathological observations. Grade IV is the most aggressive and may penetrate, proliferate, and exist in an undifferentiated, difficult-to-treat form [3, 4]. GBM is an uncommon kind of tumor with a worldwide incidence of 10 per 100,000 persons regardless of age [5]; however, males are more likely than women to get brain tumors [6]. Temozolomide (TMZ), an imidazotetrazine derivative of dacarbazine, is a first-line drug for the treatment of patients with GBM [7]. TMZ is given via oral and intravenous routes. The marketed formulations of Temozolomide (TMZ) are capsule (Temodal Capsules (100 mg/Capsule), Temoside (100 mg/capsule) and injection formulations (Temodar for injection (100 mg/vial), the specific dose of TMZ varies depending on the treatment regimen, but it is typically given in daily doses ranging from 75 to 150 mg/m^2. Most tumor cells are innately resistant to TMZ at pharmacotherapeutic doses or quickly develop resistance. Further, due to the overexpression of MGMT, 50% of TMZ-treated patients do not respond to this treatment [7]. On administration, TMZ spontaneously converts into 5-(3-methyltriazen-1-yl) imidazole-4-carboxamide (MTIC) form at physiological pH by releasing the $–CO_2$ from the imidazotetrazine ring, a six-membered ring that further gets open to convert into MTIC [8]. MTIC form is unstable and converts into AIC, resulting in the release of methyl diazonium ions (Fig 1). The cation reacts with the nucleophile site and performs the methylation at the DNA to induce autophagy [9]. TMZ is a potent anticancer drug with 100% oral bioavailability [10] and causes apoptosis via autophagy [11]. There are several limitations associated with TMZ viz., short half-life (1.8 h) [12], rapid metabolism at physiological pH (>7.0) [9], only 1% of the administered dose reaches the brain in intact form, hydrophilicity, and development of chemo-resistance [13]. Attempts have been made to improve the TMZ efficacy using nanocarrier-mediated delivery approaches. Several nanocarriers viz., liposomes, solid lipid nanoparticles, polymer-drug conjugate, and polymeric micelles were screened in recent research

[14]. The water solubility of the TMZ limits the loading efficiency into the hydrophobic core of nanocarriers, making it difficult to achieve therapeutic outcomes.

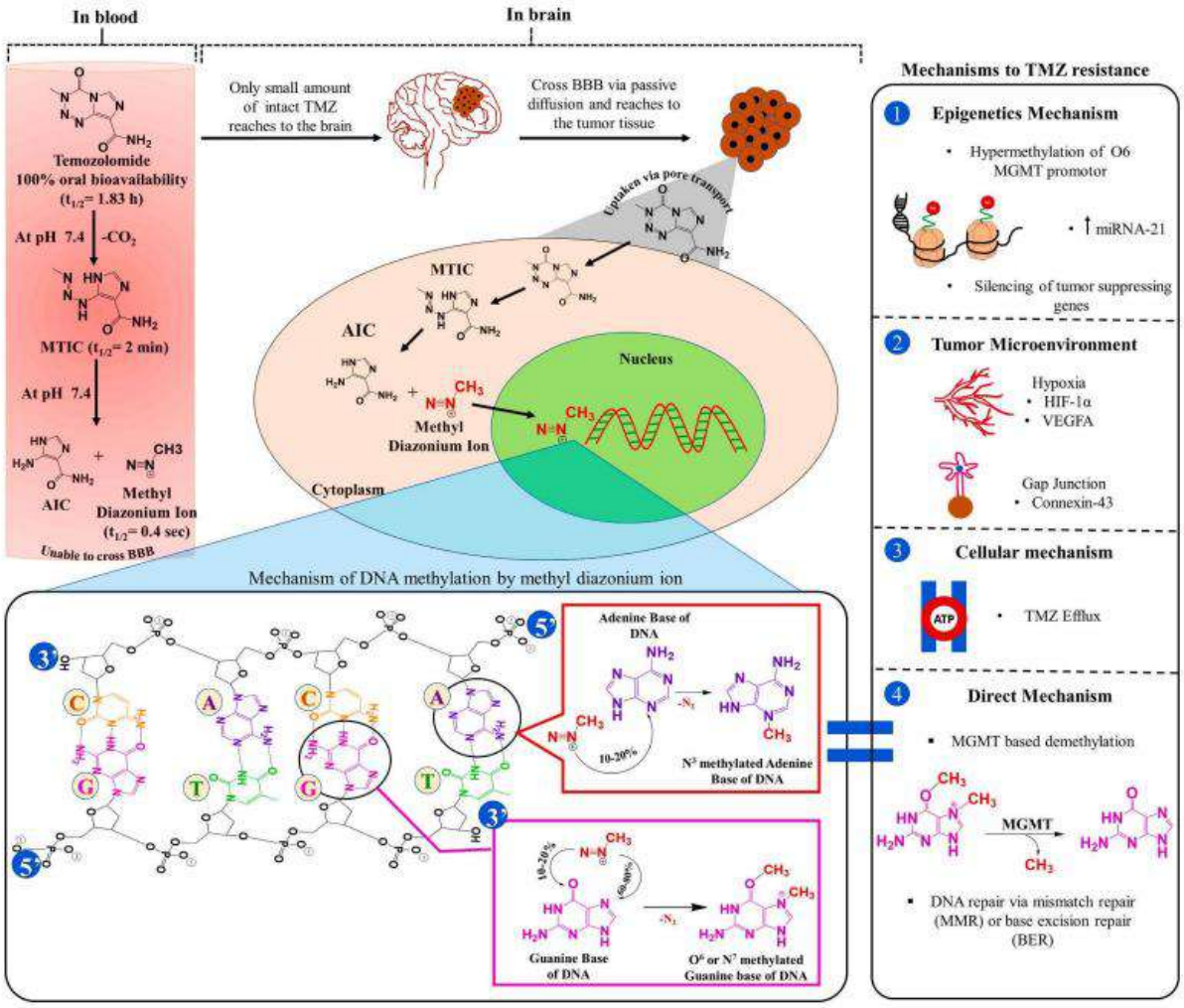

Figure 1. The fate of TMZ in the bloodstream after administration and in glioma cells after reaching the brain. Different mechanisms of TMZ resistance, 1) Epigenetic mechanism, 2) Tumor microenvironment, 3) cellular mechanism, and 4) Direct mechanism.

In 2015, Gao et al. prepared TMZ-loaded liposomes by the conventional proliposome method. The prepared nano formulation showed a narrow range particle size of 156.70 ± 11.40 nm with a PDI of 0.29 ± 0.04. The reported encapsulation efficiency was 35.45 ± 1.48% at a theoretical loading of 2.81 ± 0.20% w/w [15]. The conjugation strategy is also important to overcome the delivery difficulties wherein TMZ was conjugated to polymers or small molecules. TMZ–Perillyl alcohol conjugate (TMZ–POH) is a new TMZ analog synthesized by conjugating TMZ with POH, a naturally occurring monoterpene that enhances TMZ's cytotoxicity in several cancers [16,17].

According to Song et al., TMZ-POH suppressed MGMT that was dependent on the proteasomal pathway, and this inhibition was a key contributor to the improvement in its overall efficiency [16]. Ward et al., synthesized a polymer (methacryloyloxyethyl phosphorylcholine) using reversible addition-fragmentation chain-transfer (RAFT) polymerization and conjugated it with TMZ using a disulfide linker. The resulting polymer-TMZ conjugate enhanced TMZ stability in terms of half-life to the extent of 19 folds, along with improved cytotoxicity in glioma cells [18]. In 2020, Du et al. reported a novel conjugate of TMZ with doxorubicin [19] to exert a synergistic effect on conformational changes in the DNA (Fig 2). A nanocarrier containing copper-bound apoferritin was developed with 83% w/w loading efficiency for TMZ-DOX conjugate [19]. Further, Peng et al. developed a folate-targeted triblock polymer (Fa-PEG-PEI-PCL, Fa-PEC) and loaded TMZ along with surface decoration with siRNA targeting BCL-2 [20]. The nano carrier-based approaches collectively showed a better effect than the free TMZ. Fatty acids are saturated or unsaturated long-chain hydrocarbons with a –COOH terminal group. In addition, they possess other properties such as antioxidant, anticancer, antiproliferative action, etc. Recently, fatty acids have been used to make prodrugs by conjugating them with small molecules [21]. We have earlier reported lisofylline-linoleic acid conjugate for the treatment of diabetes mellitus. The outcomes of the study showed that the conjugate had self-assembling potential with modified pharmacokinetic properties (5-fold) [22]. Ke et al. reported a linoleic acid-conjugated paclitaxel, which enhanced the anticancer, and anti-proliferative potential along with brain tumor targeting via improving BBB permeability. Further, the conjugate showed higher cellular uptake due to the inhibition of p-gp efflux, improved in vivo kinetic behavior, and antitumor efficacy in tumor-bearing animals [23]. Fatty acids were also explored for their MGMT depletion property, for example, Goder et al. stated that lipoic acid downregulated MGMT expression and induces an autophagy-like response in colorectal tumor cells [24]. In the current study, we have synthesized TMZ-fatty acid conjugates ($6R_{1\text{-}3}$), namely TMZ-oleic acid (TOA, $6R_1$), TMZ-linoleic acid (TLA, $6R_2$), and TMZ-palmitic acid (TPA, $6R_3$), with a hydrazine linkage (-NH-NH-). The conjugates ($6R_{1–3}$) were thoroughly characterized using 1 H NMR spectroscopy and mass spectrometry. The purity of the conjugates ($6R_{1–3}$) was determined using RP-HPLC and further evaluated for in vitro cell culture in U87-MG and C_6 cells for cytotoxicity, cell migration, and apoptosis-inducing potential. The expression of MGMT protein was evaluated using western blotting. Further, the in vivo efficacy of ($6R_1$) was evaluated in the C_6 cells induced orthotropic rat glioma model, wherein the overall survival rate,

change in body weight, tumor load, brain weight, histological evaluation, and metastasis were evaluated.

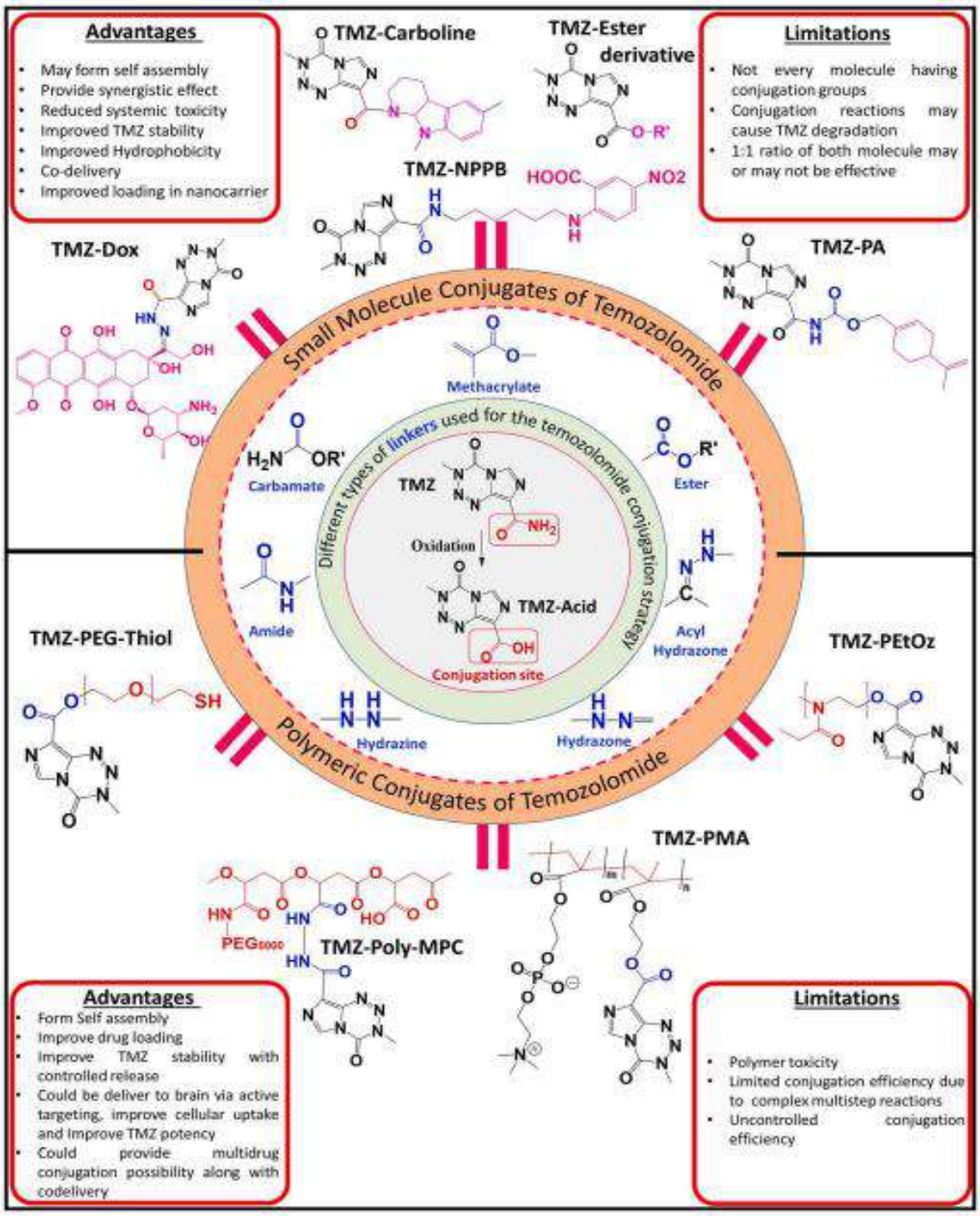

Figure 2: Conjugation strategies of Temozolomide with small molecules and polymer.

Collectively, the aim of the present study is to investigate both the physiochemical property and biological effect of the conjugates with respect to free drug. The outcomes demonstrated that fatty acid conjugates improved the physiochemical property of TMZ, such as plasma stability and hydrophobicity. Furthermore, the biological effects were also found to improve, as indicated by lower IC_{50} value and higher apoptosis, improved pharmacokinetic, and overall in vivo efficacy.

3. Objectives

a) Synthesis and characterization of temozolomide-fatty acids conjugates.
b) *In-vitro* evaluation of temozolomide-fatty acids conjugates in C_6 and U87-MG glioma cell lines
d) *In vivo* pharmacokinetics evaluation, and efficacy study of the synthesized temozolomide-fatty acid conjugate.

4. Materials

Temozolomide (TMZ) was purchased from Carbanio, India. Oleic acid, Linoleic acid, and Palmitic acid were purchased from ACME synthetic chemicals (India). Acetyl chloride, Hydrazine hydrate (80%), and N, N-diisopropylethylamine (DIPEA) were purchased from TCI Chemicals India Pvt. Ltd. (Chennai, India). N-(3-Dimethylaminopropyl)-N′-ethyl carbodiimide hydrochloride (EDC.HCl) and Hydroxy benzotriazole (HOBt) were purchased from Spectrochem Ltd. (Mumbai, India). Dulbecco's Modified Eagle's medium (DMEM), Fetal Bovine Serum (FBS), BCA kit, Annexin V Alexa fluor 488 conjugates, and annexin binding buffer were purchased from Thermo Fisher Scientific (MA, USA). 3-(4,5-dimethyl-thiazol-2-yl)-2,5-diphenyl tetrazolium bromide (MTT) was purchased from Sisco Research Laboratories (Mumbai, India). Bovine Serum Albumin (BSA), Dimethyl Sulfoxide (DMSO), and Phosphate Buffered Saline (PBS) pH 7.4 were purchased from Hi-Media Laboratories. All other reagents and solvents used in this research were purchased from local vendors.

5. Methodology

5.1 Synthesis and characterization of TMZ-acid (2)

A previously reported method was used to convert the amide group (-CO-NH_2) of TMZ (1) to a free –COOH end group [19] (Fig. 3). Briefly, TMZ (1.0 g) (1) was dissolved in 8 mL of concentrated sulphuric acid (H_2SO_4) and kept for continuous stirring for 30 min. at room temperature. Further, the reaction was transferred to a cold condition, and sodium nitrite (2.6 g) in

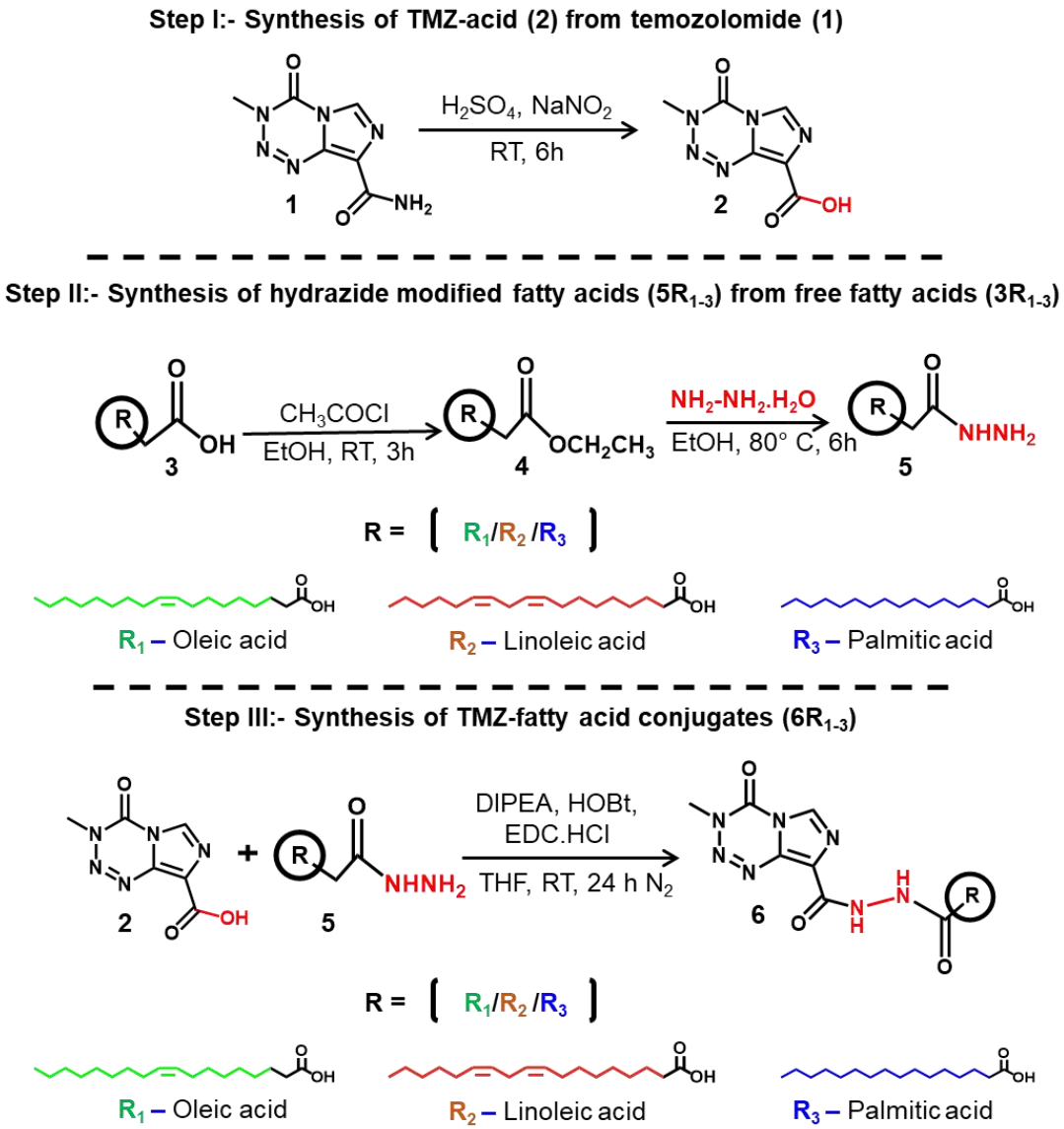

Figure 3. Synthetic scheme to obtain TMZ-fatty acid conjugates **($6R_{1-3}$)**, Step I: Hydrolysis of TMZ **(1)** to obtain TMZ-Acid **(2)**; Step II: Synthesis of hydrazide-modified fatty acids **($5R_{1-3}$)** from fatty acids **($3R_{1-3}$)**; and Step III: Synthesis of TMZ-fatty acid conjugates **($6R_{1-3}$)** by coupling TMZ-Acid **(2)** and hydrazide modified fatty acids **($5R_{1-3}$)** by the means of EDC/HOBt reaction.

11.2 mL water was added dropwise under continuous nitrogen purging. The resulting solution was kept on stirring at room temperature overnight, which was followed by the addition of 10 mL of ice-cold water to precipitate the product. The crude TMZ-acid (2) was obtained by vacuum filtration and characterized using 1 H NMR, FT-IR, and mass spectrometry.

5.2. Synthesis of the hydrazide-modified fatty acids ($5R_{1–3}$)

A two-step chemical reaction was adopted for the -COOH end group modification of fatty acid to hydrazide (− NH− NH_2) group. Firstly, the fatty acid (1.0 g) ($3R_{1–3}$) was dissolved in 15 mL of dry ethanol and kept on stirring for 10 min. at room temperature. Further, 500 µL of acetyl chloride was added dropwise to the reaction mixture and kept for 3 h at room temperature. The reaction was quenched by adding sodium bicarbonate (2.0 g), followed by celite filtration to get the crude esterified fatty acid ($4R_{1–3}$). The resulting product was directly used in the next reaction to obtain a hydrazide-modified fatty acid ($5R_{1–3}$) (Fig. 3). Briefly, 800 mg of the esterified fatty acid ($4R_{1–3}$) in 15 mL of dry ethanol was taken in a 50 mL round-bottom flask, followed by the addition of 1 mL of 80% hydrazine hydrate dropwise at room temperature. Further, the reaction was refluxed for 6 h and monitored using TLC with a solvent system comprising ethyl acetate and hexane (50:50). The reaction was quenched by adding 15 mL of ice-cold water, and the product was extracted using ethyl acetate. The organic layer was separated, dried over sodium sulfate, and concentrated using a rotary evaporator to get a yellow/whitish semisolid hydrazide-modified fatty acid ($5R_{1–3}$). The same protocol was utilized to synthesize all three hydrazide-modified fatty acids ($5R_1$, $5R_2$, and $5R_3$). The resulting products were characterized using 1H NMR spectroscopy and mass spectrometry.

5.3. Synthesis of TMZ-fatty acid conjugates ($6R_{1–3}$)

The TMZ-fatty acid conjugates ($6R_{1–3}$) were synthesized using EDC/ HOBt-mediated amide coupling between TMZ-acid (2) and hydrazide-modified fatty acids ($5R_{1–3}$). Briefly, TMZ-acid (2) (500 mg) and fatty acid hydrazide ($5R_{1-3}$) (~800 mg) were dissolved in tetrahydrofuran (THF, 10 mL) followed by the addition of DIPEA (400 µL), and the reaction was stirred at room temperature for 15 min. to activate the –COOH group of TMZ-acid (2). Thereafter, the reaction mixture was kept at 0°C and HOBt (346 mg) followed by EDC.HCl (476.81 mg) in 5 mL of THF was subsequently added and the mixture was stirred at room temperature for 24 h under an inert atmosphere of nitrogen. After this, 20 mL of ice-cold water was added to the reaction mixture, and the desired product was extracted using dichloromethane (DCM). The organic layer was separated, dried over anhydrous $NaSO_4$, and concentrated using a rotary evaporator to obtain crude products. Further, TMZ-Fatty acid conjugates ($6R_{1–3}$) were purified by column chromatography using DCM and methanol as mobile phase in a ratio of 95:05. The final products ($6R_{1–3}$) were characterized

using 1H NMR spectroscopy, and mass spectrometry. The purity of the conjugates was determined by using RP-HPLC with a mobile phase comprising ACN/MilliQ (0.1% formic acid) in a proportion of 95:05.

5.4. Cell culture assays

Glioma cells (C_6 and U87-MG) were obtained from the National Centre for Cell Science (NCCS, Pune) and were maintained in Dulbecco's Modified Eagle's medium (DMEM) supplemented with 10% fetal bovine serum (FBS) and 1% penicillin/streptomycin antibiotics under a humid environment at 37°C with 5% CO_2. The cells were allowed to grow up to 80% confluency before seeding for experimentation.

5.5. Cytotoxicity assay

C_6 or U87-MG glioma cells were seeded in a 96-well culture plate with a density of 5×10^3 cells/well and allowed to grow overnight in a humid environment with 5% CO_2 at 37°C temperature. Afterward, cells were treated with 25 uM to 1000 μM concentration of free TMZ, free OA, free LA, free PA, TMZ + OA, TMZ + LA, TMZ + PA, TOA ($6R_1$), TLA ($6R_2$), and TPA ($6R_3$) in 0.05% DMSO. Herein, cells treated with 0.05% DMSO in DMEM media were taken as the negative control. After treatment, cells were incubated for 72 h followed by the replacement of media with fresh DMEM media containing 0.5 mg/mL of 3-(4,5- dimethyl thiazolyl-2)-2,5-diphenyl tetrazolium bromide (MTT) and incubated for 4 h. Further, the MTT-containing media was discarded, and 200 μL of dry DMSO was added to each well to dissolve the formazan crystals. The metabolic activity of cells as a function of cell viability was determined by reading the absorbance at 630 nm using an Epoch microplate spectrophotometer (Biotek Instruments, USA). Herein, the absorbance at 630 nm was subtracted from the absorbance at 570 nm to minimize the background absorbance. The following formula was used to determine the % viability [25].

$$\% \text{ Cell viability} = \frac{\text{OD (570 − 630 nm) of treatment group}}{\text{OD (570 − 630 nm) of control group}} \text{ X } 100$$

5.6. Migration assay

Briefly, C_6 or U87-MG cells were seeded in 6 well plates and incubated overnight. The next day, the straight-line scratch was made in the monolayer of the cells, and then the debris was removed by washing thrice with PBS followed by the addition of fresh media containing TMZ, TOA, TLA,

and TPA with concentrations equivalent to their respective IC_{50} values. Herein, the untreated cells, added with DMSO only, were taken as a negative control. After 48 h, the cells were observed under a microscope (Zeiss, Germany) for tracking the migration of the cells in the scratched area and compared with negative control cells.

5.7. Apoptosis assay

For the analysis of the apoptotic status of C_6 and U87-MG cells treated with TMZ (1) and its fatty acid conjugates ($6R_{1–3}$), an Annexin V/PI kit-based flow cytometry assay was performed. Briefly, C_6 or U87- MG glioma cells were seeded in 6 well plates with a density of 1×10^5 cells/well followed by overnight incubation at 37°C with 5% CO_2 in a humid environment. Further, the cells were incubated with different treatments i.e., free TMZ, TMZ + OA, TMZ + LA, TMZ + PA, TOA ($6R_1$), TLA ($6R_2$), and TPA ($6R_3$) in 0.05% DMSO for 24 h at their respective IC_{50}. Herein, cells treated with DMSO were taken as a negative control. The cells were trypsinized, centrifuged, and redispersed in Annexin binding buffer followed by the addition of Annexin V/PI, incubated for 5 min in the dark, and analyzed using flow cytometry (CytoFlex, Beckman Coulter, USA). Data were interpreted using CytExpert 3.0 software [26].

5.8. Western blotting

Briefly, C_6 or U87-MG cells were seeded in a petri dish with a density of 5×10^5 followed by incubation at 37°C/5% CO_2 under a humid environment. The next day, the cells were treated with free TMZ, TOA ($6R_1$), TLA ($6R_2$), and TPA ($6R_3$) in 0.05% DMSO with a concentration equivalent to their IC_{50} value and incubated for 48 h. Ice-cold RIPA buffer along with protease inhibitor was used to extract the protein from C_6 or U87-MG cells. The protein concentration was determined using a BCA kit (Thermo Scientific, USA), and 25 μg of total protein was loaded and resolved in 12% SDS-PAGE at 95 V for 1.5 h. The protein bands were transferred to nitrocellulose membrane followed by incubation with primary antibody (MGMT, GAPDH) overnight at 4°C. The membrane was washed with TBST buffer and incubated with 1:1000 times diluted secondary antibody for 1 h at room temperature. Further, the Pierce™ ECL Western Blotting Substrate (Thermo Scientific, USA) was poured over the membrane and observed under the ChemiDoc system (Bio-Rad, USA).

5.9. Plasma stability study

The plasma stability study of the TMZ and its fatty acid conjugates ($6R_{1–3}$) was evaluated using a previously reported HPLC-based method with slight modification [27]. Firstly, a stock solution of 30 mg/mL of TMZ (1), TOA ($6R_1$), TLA ($6R_2$), and TPA ($6R_3$) was prepared separately in a solvent system (5% dimethylacetamide (v/v), 10% ethanol (v/v), and 5% tween 80 (w/v)). Further, 3 mL of fresh rat plasma was taken in a 5 mL glass vial, and 100 µL of TMZ (1), TOA ($6R_1$), TLA ($6R_2$), and TPA ($6R_3$) from the stock was spiked. Next, the samples were kept under stirring at 37 °C temperature, and 100 µL of plasma was taken after predetermined time points (0, 0.25, 0.5, 1, 2, 4, 6, 8, 12, and 24 h). The collected plasma samples were acidified by adding 5 µL of 0.1 mM of ascorbic acid, followed by the addition of 900 µL of ACN. The resulting samples were vortexed for 3 min followed by centrifugation at 10,000 rpm for 30 min. The supernatant was collected, vacuum dried, and resuspended in the mobile phase (ACN: Acetate buffer, 95:05), and analysis was done using HPLC based method. The data was presented as % drug remaining, and the concentration at t_0 was considered as 100%

5.10. Development of C_6 cells induced orthotropic glioblastoma in Sprague Dawley rats

For orthotropic glioma model development, Sprague Dawley (SD) rats were used after the approval of protocol from the Institutional Animal Ethics Committee (IAEC) of BITS Pilani, Pilani Campus (Protocol number: IAEC/RES/29/04). All the experimental procedures were carried out in accordance to the guidelines of the Committee for the Purpose of Control and Supervision of Experiments on Animals (CPCSEA). To anesthetize rats (n = 05; 4–6 weeks of age), ketamine (80 mg/kg) and xylazine (4.5 mg/kg) were intraperitoneally injected, and then the head of the rats was shaved, and an incision of about 3–4 cm was made to expose the skull, followed by a burr hole at 2 mm anterior and 3 mm lateral to the bregma. The rat was fixed with a stereotaxic apparatus, and 2×10^6 of C_6 cells suspended in 10 µL of PBS were injected through the burr hole using Hamilton's syringe at a flow rate of 3 µL/min at a depth of 4 mm. The burr hole was sealed using biodegradable wax, and the incision was sutured [28]. Animals were placed back in the home cages and were kept under physical and behavioral observations as an indication of tumor development.

5.11. Pharmacokinetic study

Briefly, SD rats bearing C_6 cells-based orthotropic glioma tumors were randomly divided into four groups (n = 04), namely TMZ (1) and TOA ($6R_1$), treated with 25 mg/kg of dose. For the injection, free TMZ (1) was dissolved in the normal saline, and TOA was dissolved in the 5% dimethylacetamide(v/v), 10% ethanol (v/v), and 5% Tween 80 (w/v) in normal saline and injected intravenously. At predetermined time points (i.e., 0.25, 0.5, 0.75, 1, 2, 4, 6, 8, 12, 24, and 48 h), 200 μL of blood was collected in EDTA containing microcentrifuge tubes followed by centrifugation at 10,000 rpm for 10 min to collect the plasma. The plasma was acidified immediately using 5 uL of 0.1 M ascorbic acid, and TMZ (1) and its fatty acid conjugate ($6R_1$) were extracted from the plasma by liquid-liquid extraction method. Firstly, 50 μL of plasma was taken and 5 μL of 0.1 M ascorbic acid was added into it and mixed thoroughly after the addition of IBMX (5 μL of 250 ng/mL; internal standard) and vortexed for 15 min. After that, 1.2 mL of tertiary butyl methyl ether (TBME) was added, and the mixture was vortexed for 3 min, followed by centrifugation for 4 min at 10000 rpm. The organic layer (1 mL) was separated and evaporated to dryness to obtain a residue. The residue was reconstituted in 100 μL of the mobile phase (A: 10 mM Ammonium Acetate +0.1% Formic Acid; B: Methanol+0.1% Formic Acid), and 10 μL was injected into LC-MS/MS system (Waters, Xevo TQD). Phoenix 2.1 Winolin software was used to determine various pharmacokinetic parameters viz., $t_{1/2}$ (half-life), C_{max} (maximum plasma concentration), $AUC_{0\text{-}t}$, and $AUC_{0\text{-}\infty}$, MRT (mean residence time), V_d (volume of distribution) and C_L (clearance) by using the non-compartment model approach.

5.12. Efficacy study

Briefly, after glioma cell inoculation, animals were kept for 7 days and randomly divided into three groups (n = 05), namely positive control (PBS treated), free TMZ treated, and TOA ($6R_1$) treated group. The animals were treated thrice a week with a 10 mg/kg dose of TMZ (in normal saline) or TOA ($6R_1$) (in normal saline containing 5% Dimethylacetamide(v/v), 10% ethanol (v/v), and 5% tween 80 (w/v)) via the intravenous route. The positive control animal received normal saline containing 5% dimethylacetamide (v/v), 10% ethanol (v/v), and 5% Tween 80 (w/v) administered via the intravenous route. The animals were monitored continuously for their body weight, locomotion activity, and overall health score for 80 days. Further, the brain of all animals was isolated and examined for physical appearance, total weight (g), hemisphere width (mm), and

histological characteristics. The lungs of the animals were collected and fixed with Bouin's solution (75% picric acid, 25% formalin, 5% glacial acetic acid) for 6 h followed by incubation in 70% alcohol to examine the metastasis of glioma within the lungs.

6. Results

6.1. Synthesis and characterization of TMZ-Acid (2)

Dropwise addition of $NaNO_2$ to a TMZ solution in H_2SO_4 resulted in the synthesis of TMZ-acid (2) as a white floppy powder with >80% practical yield. Characterization of the synthesized TMZ-

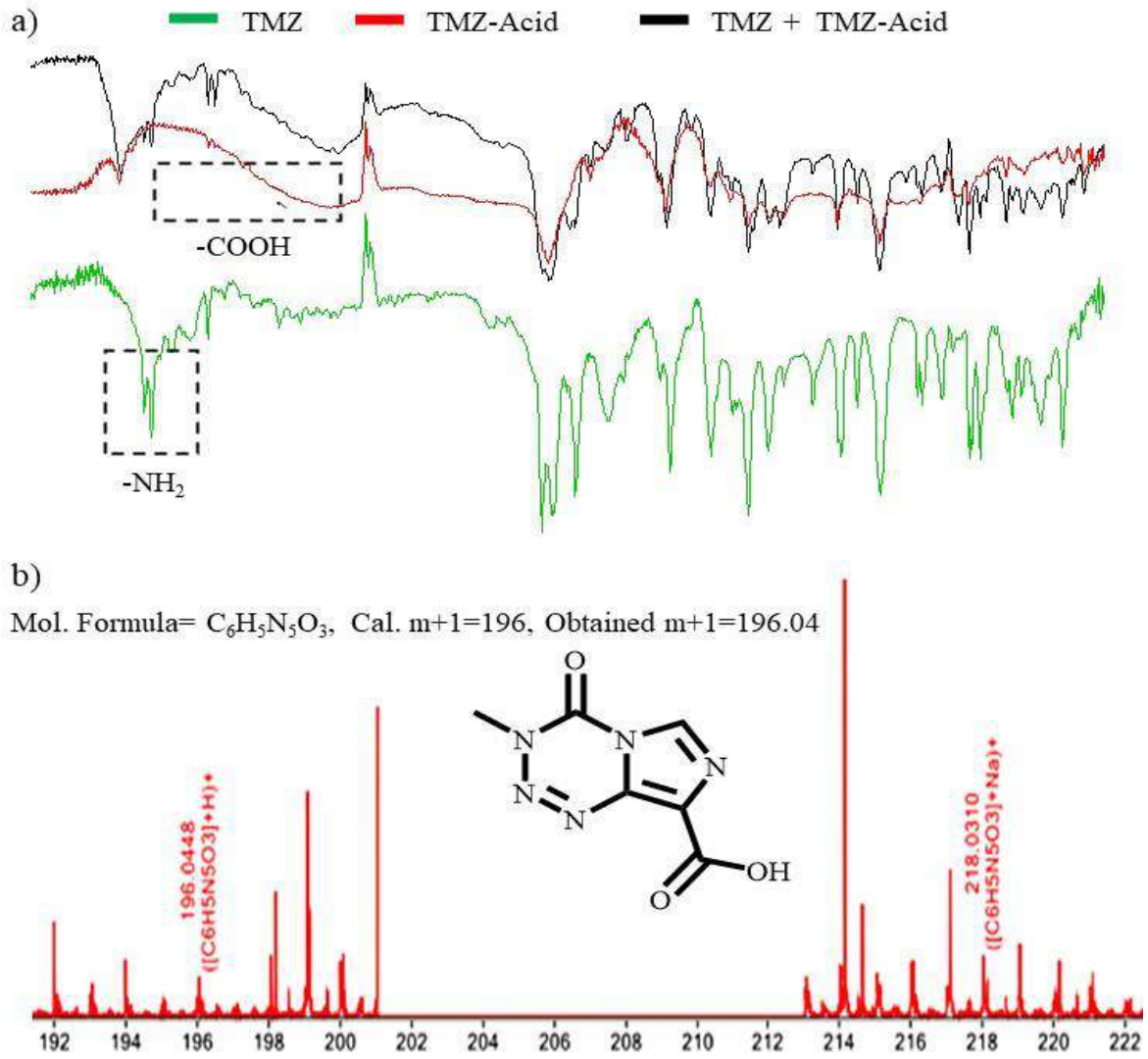

Figure 4 . Characterization of acid derivative of TMZ *i.e* TMZ-acid **(2)**, a) FTIR spectra, and b) ESI-TOF mass spectrometry peak.

acid was done using FT-IR spectroscopy, where the disappearance of the –NH_2 peak of amide at 3300–3500 cm^{-1} and the appearance of –OH peak of carboxylic acid at 2700–3300 cm^{-1} confirmed the synthesis of TMZ-acid (2) (Fig. 4a). Additionally, the mass of the TMZ-acid (2) was determined as a final confirmation where a [M + 1]+ peak at 196.0448 ($C_6H_5N_5O_3$, Cal. [M + 1]+ = 196.0470) was observed (Fig. 4b).

6.2. Synthesis and characterization of the hydrazide-modified fatty acids ($5R_{1–3}$)

The free-COOH end group of the fatty acids ($3R_1$, $3R_2$, and $3R_3$) could be used as a potential site for conjugation with other moieties. Esterification of the free–COOH was performed with acetyl chloride to get yellowish, oily esterified fatty acids ($4R_{1–3}$) with a practical yield >90%. The

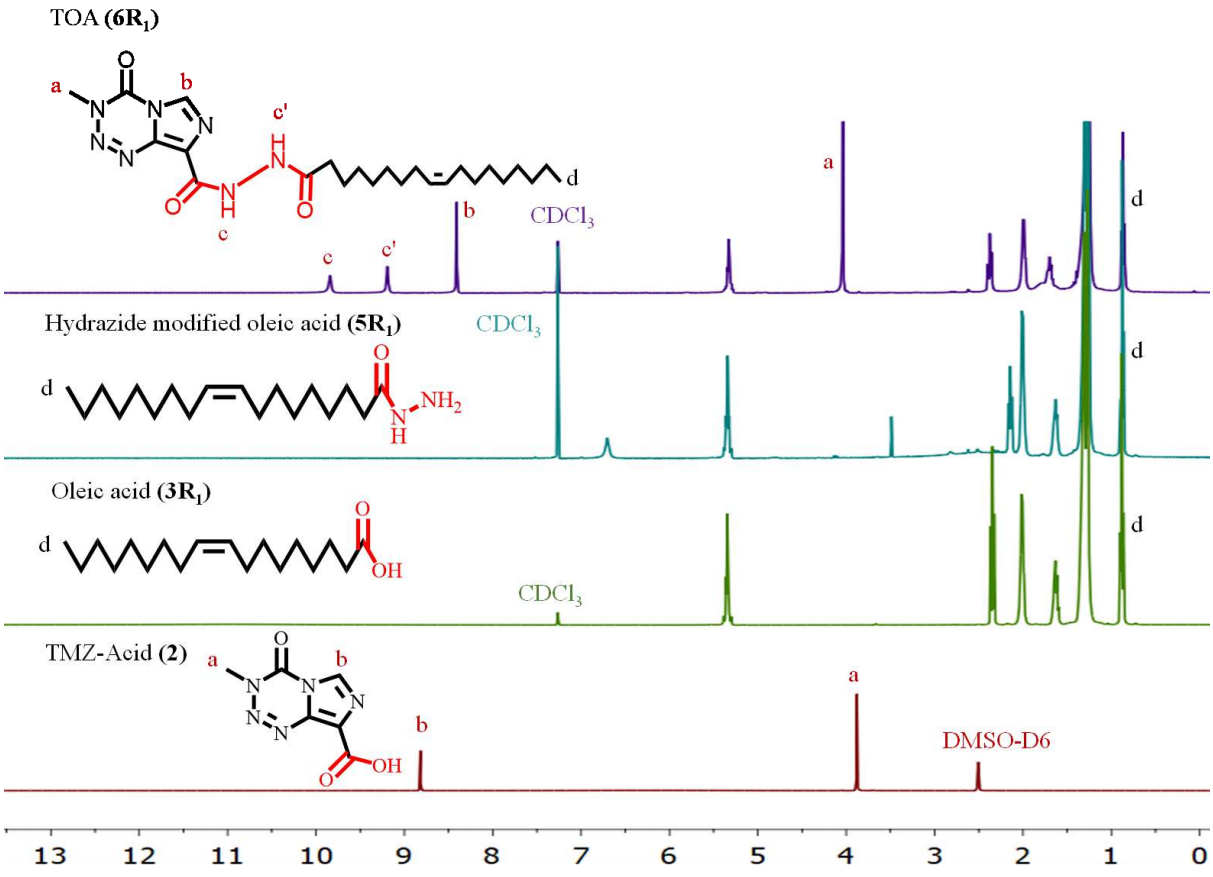

Figure 5. ^{1}H NMR spectra of oleic acid **($3R_1$)**, hydrazide-modified oleic acid **($5R_1$)**, TMZ-Acid **(2),** and TOA **($6R_1$)** conjugate.

resulting product was modified to get a yellow-colored semisolid product with an 85% practical yield. Fig. 5 showed hydrazide-modified oleic acid [1 H NMR (400 MHz, CDCl3) δ 6.73 (brs,

1H), 5.41–5.31 (m, 2H), 2.17 (d, J = 7.6 Hz, 2H), 2.07–1.97 (m, 4H), 1.71–1.59 (m, 2H), 1.37–1.25 (m, 20H), 0.90 (t, J = 6.8 Hz, 3H)]. Fig. 6 showed hydrazide-modified linoleic acid [1 H NMR (400 MHz, CDCl3) δ 7.12 (brs, 1H), 5.42–5.26 (m, 4H), 2.76 (t, J = 6.4 Hz, 2H), 2.15 (t, J = 8.0 Hz, 2H), 2.08–2.00 (m, 2H), 1.68–1.56 (m, 2H), 1.40–1.27 (m, 16H), 0.89 (t, J = 6.8 Hz, 3H)]. Fig. 7 showed hydrazide-modified palmitic acid [(400 MHz, CDCl3) δ 3.67 (brs, 3H), 2.31 (t, J = 7.6 Hz, 2H), 1.68–1.55 (m, 2H), 1.34–1.24 (m, 24H), 0.89 (d, J = 7.2 Hz, 3H)], wherein the peak at 4.20–4.03 (m, 2H) and δ 7.12–7.30 (brs, 1H) confirmed the presence of hydrazine end group. Further, mass spectrometry ESI-TOF for hydrazide-modified linoleic acid (Mol. Formula $C_{18}H_{34}N_2O$; Cal. [M + 1]+ = 295.3; obtained [M + 1]+ = 295.28), for hydrazide-modified oleic

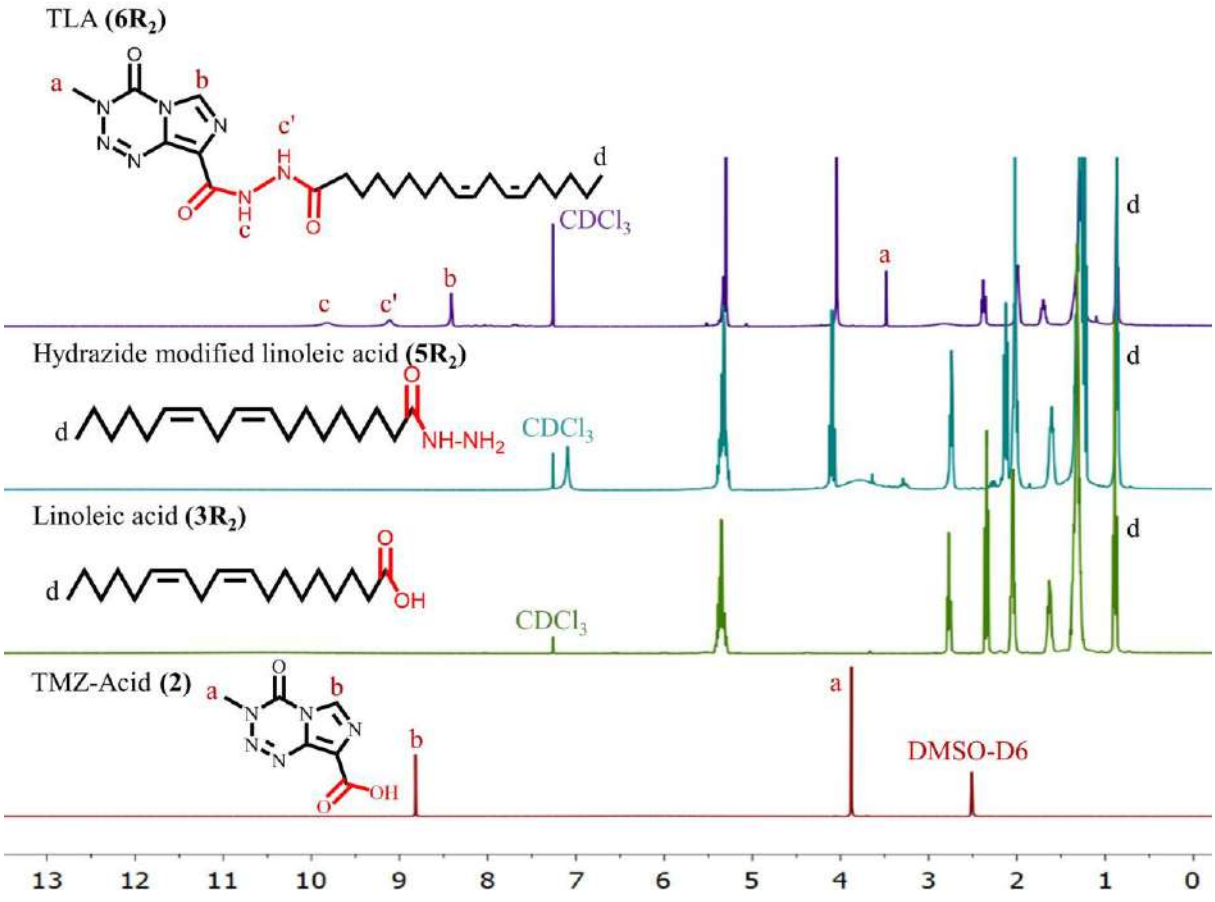

Figure 6. Characteristic ^{1}H NMR spectra of linoleic acid **(3R$_2$)**, hydrazide derivative of linoleic acid **(5R$_2$)**, TMZ-Acid **(2)** and TLA (6R$_2$) conjugate.

acid (Mol. formula- $C_{18}H_{36}N_2O$; Cal. [M + 1]+ = 297.3; obtained [M + 1]+ = 297.28) and for hydrazide modified palmitic acid (Mol. formula- $C_{16}H_{34}N_2O$; Cal. [M + 1]+ = 271.27; obtained [M + 1]+ = 271.27) confirmed the successful synthesis of hydrazide modified fatty acids.

6.3. Synthesis and characterization of TMZ-fatty acid conjugates ($6R_{1–3}$)

TMZ-Acid (2) and hydrazide-modified fatty acids ($5R_{1–3}$) were conjugated using EDC/HOBt-mediated amide coupling chemistry. The reaction was monitored using TLC with a solvent system containing DCM: MeOH (95:05), and the appearance of a bright yellow spot on TLC indicated the completion of the synthesis of the conjugate. The final product was purified using column

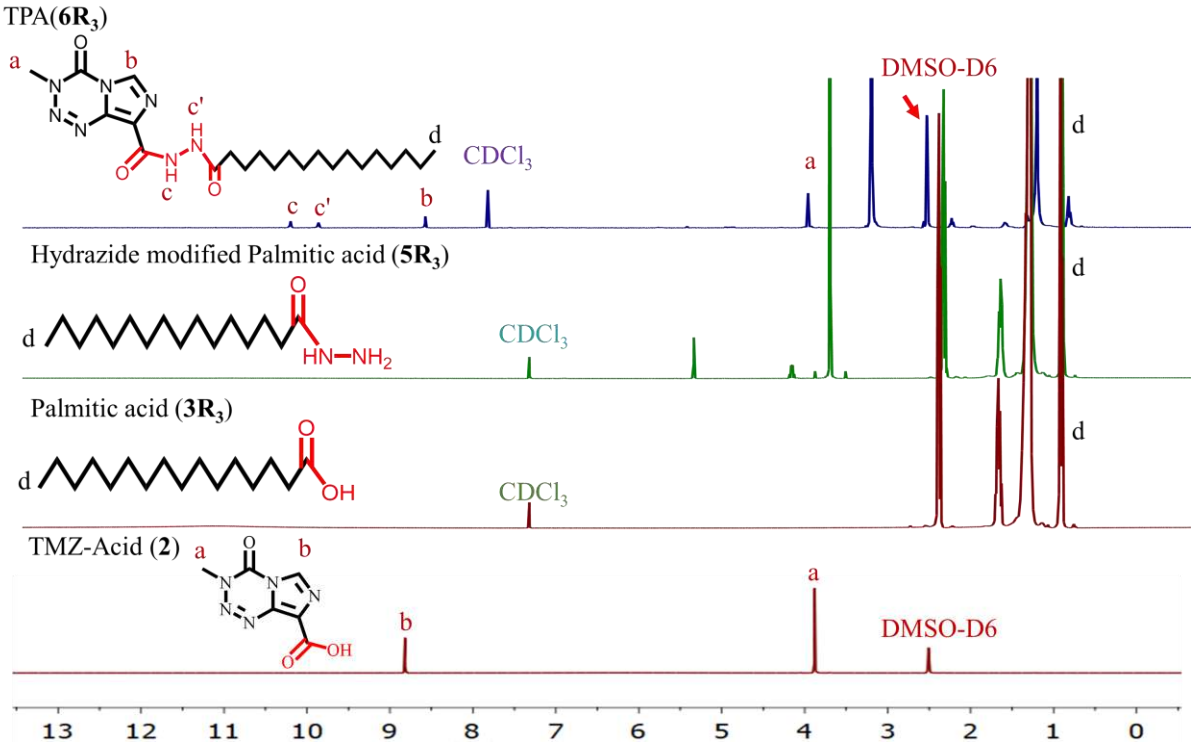

Figure 7. ^{1}H NMR spectra of palmitic acid **(3R$_3$)**, hydrazide-modified palmitic acid **(5R$_3$)**, TMZ-COOH **(2),** and TPA **(6R$_3$)** conjugate.

chromatography with DCM: MeOH (95:05) as the mobile phase. The final yield of TOA ($6R_1$), TLA ($6R_2$), and TPA ($6R_3$) was 0.728 g (72%), 0.720 g (72%), and 0.500 g (50%), respectively. However, the conjugation reaction showed good reproducibility in terms of the final yieldobtained. Fig. 5 showed 1 H NMR spectra of TOA ($6R_1$) [1 H NMR (400 MHz, CDCl3) δ 9.86 (brs, 1H), 9.22 (brs, 1H), 8.43 (s, 1H), 5.39–5.30 (m, 2H), 4.06 (s, 3H), 2.40 (t, J = 7.2 Hz, 2H), 2.06–1.97 (m, 4H), 1.77–1.64 (m, 2H), 1.37–1.24 (m, 20H), 0.89 (t, J = 6.4 Hz, 3H)]. Fig. 6 showed 1 H

NMR spectra of TLA (6R2) [1 H NMR (400 MHz, CDCl3) δ 9.83 (brs, 1H), 9.14 (brs, 1H), 8.44 (s, 1H), 5.38–5.30 (m, 4H), 4.07 (s, 3H), 2.40 (t, J = 7.6 Hz, 2H), 2.06–1.97 (m, 4H), 1.77–1.69

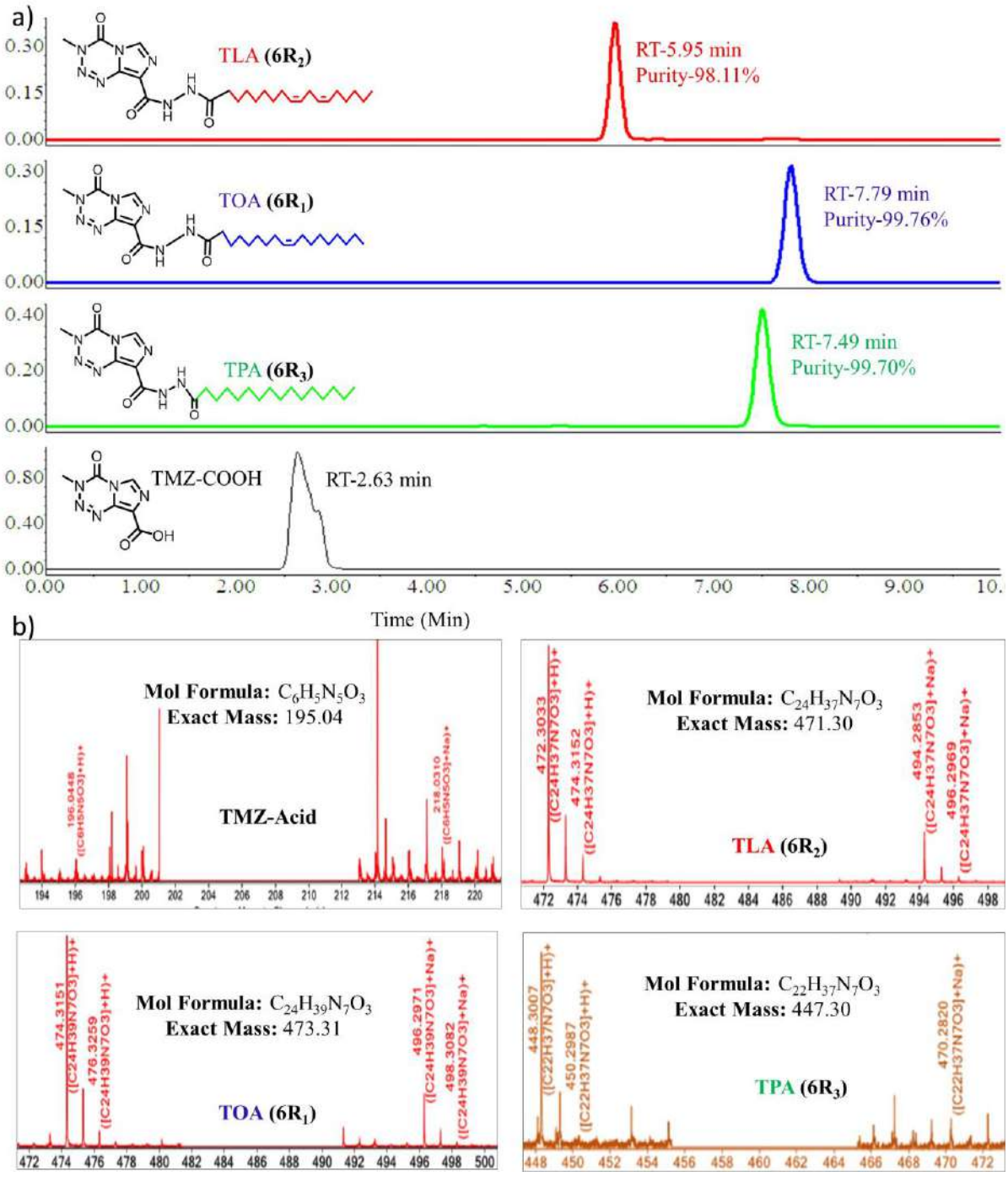

Figure 8. Characteristics HPLC and mass spectra (HRMS) of TOA **(6R1)**, TLA **(6R2),** TPA **(6R3)** conjugates, and TMZ-Acid **(2)**.

(m, 2H), 1.35–1.24 (m, 16H), 0.89 (t, J = 6.8 Hz, 3H)]. Fig. 7 showed 1 H NMR spectra of TPA ($6R_3$) [1 H NMR (400 MHz, CDCl3, DMSO-d6) δ 10.15 (brs, 1H), 9.82 (brs, 1H), 8.53 (s, 1H), 3.93 (s, 3H), 2.21 (t, J = 7.4 Hz, 2H), 1.63–1.52 (m, 2H), 1.27–1.13 (m, 24H), 0.81 (t, J = 6.8 Hz, 3H)]. The TMZ peaks at δ 4.0–4.2 (a, -CH_3, s, 3H), δ 8.2–8.5 (b, -CH, s, 1H), and hydrazide linker peaks at δ 9.0–9.2 (c', -NH, s, 1H), δ 9.7–10.5 (c, -NH, s, 1H) showed successful conjugation. Further, mass spectrometry data (Fig. 8b) of TOA ($6R_1$) (Mol. formula. $C_{24}H_{39}N_7O_3$; Cal. [M + 1]+ = 474.3192; obtained [M + 1]+ = 474.3151), TLA (6R2) (Mol. formula. $C_{24}H_{37}N_7O_3$; Cal. [M + 1]+ = 472.3036; obtained [M + 1]+ = 472.3033), and TPA ($6R_3$) (Mol. formula. $C_{22}H_{37}N_7O_3$; Cal. [M + 1]+ = 448.3036; obtained [M + 1]+ = 448.3007) confirmed the synthesis of the conjugates. The purity of conjugates were determined using an RP-HPLC system with a mobile phase comprising ACN/water (0.1% formic acid) in a proportion of 95:05, wherein all three conjugates showed a purity of >98% (Fig. 8a).

6.4. Cytotoxicity and migration assay

For the calculation of the % cell viability, DMSO-treated cells were taken as a negative control. Results showed that the TOA ($6R_1$), TLA ($6R_2$), and TPA ($6R_3$) conjugates had an IC_{50} value of 101.4 μM, 67.97 μM, and 672.04 μM, respectively in C_6 cells (Fig. 9 a1). However, the physical mixtures of TMZ with fatty acids, i.e. TMZ + OA, TMZ + LA, TMZ + PA, and free fatty acids ($3R_{1–3}$) i.e. free OA, free LA, and free PA showed IC_{50} of 331.88 μM, 198.34 μM, 1000 μM and 628.03 μM, 377.5 μM, 293.84 μM, respectively in C_6 cells (Fig. 9 a1). Similarly, in U87-MG cells the TOA ($6R_1$), TLA ($6R_2$), and TPA ($6R_3$) conjugates showed an IC_{50} value of 428.25 μM, 366.42 μM, and 413.69 μM, respectively (Fig. 9 b1). Further, the physical mixtures i.e. TMZ + OA, TMZ + LA, TMZ + PA, and free fatty acids ($3R_{1–3}$) i.e. free OA, free LA, and free PA showed IC_{50} of 367.99 μM, 352.2 μM, 188.58 μM, and 306.01 μM, 248.01 μM, and 289.10 μM, respectively in U87-MG cells (Fig. 9 b1). Additionally, the migration properties of C_6 and U87-MG cells were determined in the presence of TMZ (1), TOA ($6R_1$), TLA ($6R_2$), and TPA ($6R_3$). As shown in Fig. 9a2 & b2, the migration potential of both the cells was seen to be reduced significantly when cells were treated with TMZ-fatty acid conjugates ($6R_{1–3}$) as compared to the free TMZ (1).

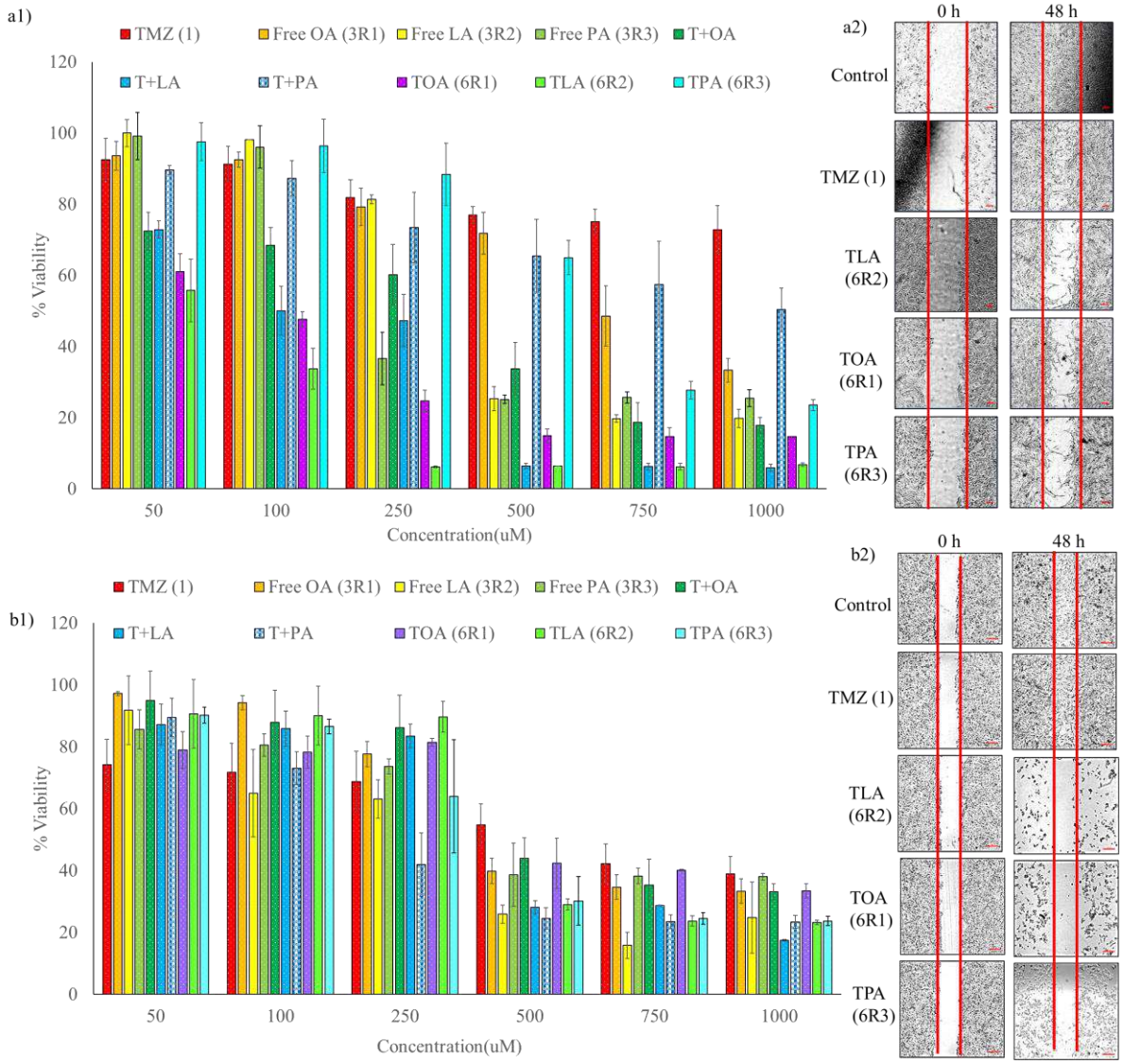

Figure 9. *In vitro* evaluation of TMZ-Fatty acid conjugates in C_6 and U87-MG cells, a1&b1) cells viability assay in C_6 and U87-MG cells respectively, and a2&b2) migration assay in C_6 and U87-MG cells respectively

6.5. Apoptosis assay

Annexin/PI staining-based flow cytometric assay was used to determine the apoptotic potential of TMZ (1), TOA ($6R_1$), TLA ($6R_2$), TPA ($6R_3$), TMZ + OA, TMZ + LA, and TMZ + PA in C_6 and U87-MG cells. Fig. 10a&b represented the apoptosis data, where C_6 cells treated with free TMZ (1) showed total apoptosis of 18.28% (early apoptosis, 4.96%; late apoptosis, 13.32%). While conjugates i.e. TOA ($6R_1$) showed 83.19% (early apoptosis, 14.32%; late apoptosis, 68.87%), TLA

($6R_2$) showed 52.2% (early apoptosis, 16.39%; late apoptosis, 35.81%), and TPA ($6R_3$) showed 63.39% (early apoptosis, 26.61%; late apoptosis, 36.78%). The physical mixture i.e. TMZ + OA

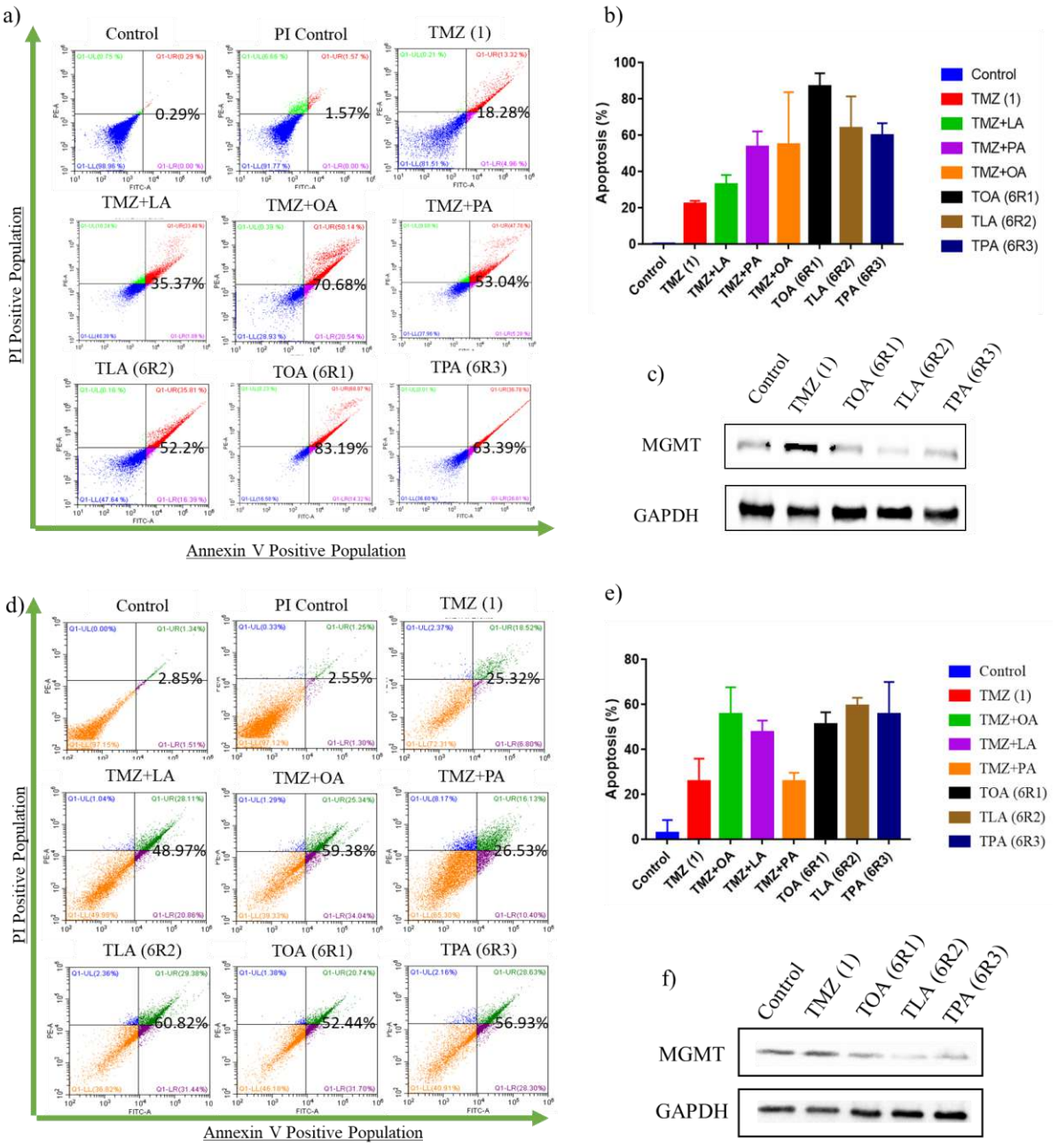

Figure 10. *In vitro* evaluation of TMZ-fatty acid **($6R_{1-3}$)** conjugates in C_6 and U87-MG cells, a&d) apoptosis status in C_6 and U87-MG cells respectively, b&e) quantitative apoptotic of C_6 and U87-MG cells respectively, and c&f) MGMT expression in C_6 and U87-MG cells respectively after different treatments.

showed 70.68% (early apoptosis, 20.54%; late apoptosis, 50.14%), TMZ + LA showed 35.37% (early apoptosis, 1.89%; late apoptosis, 33.48%) and TMZ + PA showed 53.04% (early apoptosis, 5.28%; late apoptosis, 47.76% (Fig. 10a&b). Similarly, in U87-MG cells, TMZ (1) showed apoptosis of 25.32% (early apoptosis, 6.80%; late apoptosis, 18.52%). The conjugates i.e., TOA ($6R_1$) showed 52.44% (early apoptosis, 31.70%; late apoptosis, 20.74%), TLA ($6R_2$) showed 60.82% (early apoptosis, 31.44%; late apoptosis, 29.38%), and TPA ($6R_3$) showed 56.93% (early apoptosis, 28.30%; late apoptosis, 28.63%). The physical mixtures i.e., TMZ + OA showed 59.38% (early apoptosis, 34.04%; late apoptosis, 25.34%), TMZ + LA showed 48.97% (early apoptosis, 20.86%; late apoptosis, 28.11%), and TMZ + PA showed 26.53% (early apoptosis,5

6.6. Western blotting

The expression of MGMT was determined at the protein level in both C_6 and U87-MG cell lines using the western blot analysis. As shown in Fig. 10c, the C_6 cells inherently have the expression of MGMT protein without any treatment and after treatment with free TMZ (1), the expression of MGMT was further increased. Interestingly, after the treatment with TOA ($6R_1$), TLA ($6R_2$), and TPA ($6R_3$) expression of MGMT gets reduced in the C_6 cell lines. Similarly, the U87-MG cells showed an increase in expression of MGMT after the treatment with free TMZ (1), and the expression of MGMT get reduced when the cells were treated with TOA ($6R_1$), TLA ($6R_2$) and TPA ($6R_3$) (Fig. 10f).

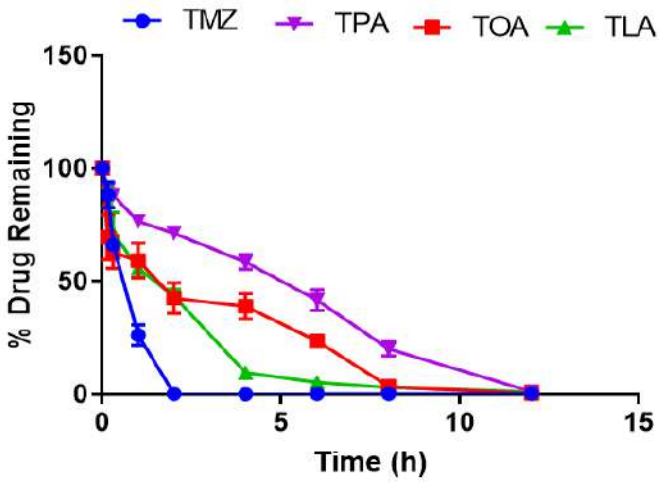

Figure 11: The stability study of TMZ **(1)** and TMZ-fatty acid conjugates **($6R_{1-3}$)** in rat plasma (n=05).

6.7. Plasma stability study

The plasma stability study was performed at a different time interval as shown in Fig. 11, the percentage of TMZ was about 26.14% after 1 h. On the other hand, the TOA ($6R_1$), TLA ($6R_2$), and TPA ($6R_3$) were found 59.21%, 55.79%, and 76.53%, respectively. After 2 h, only~0.16% of the TMZ was remaining. However, interestingly, there was 42.52%, 43.37%, and 76.53% of TOA ($6R_1$), TLA ($6R_2$), and TPA ($6R_3$), respectively, were observed. Moreover, after 6 h, the remaining % of TOA ($6R_1$), TLA ($6R_2$), and TPA ($6R_3$) was 23.6%, 5.43%, and 41.6%, respectively. However, there was no detectable amount was observed after 12 h. 4.8.

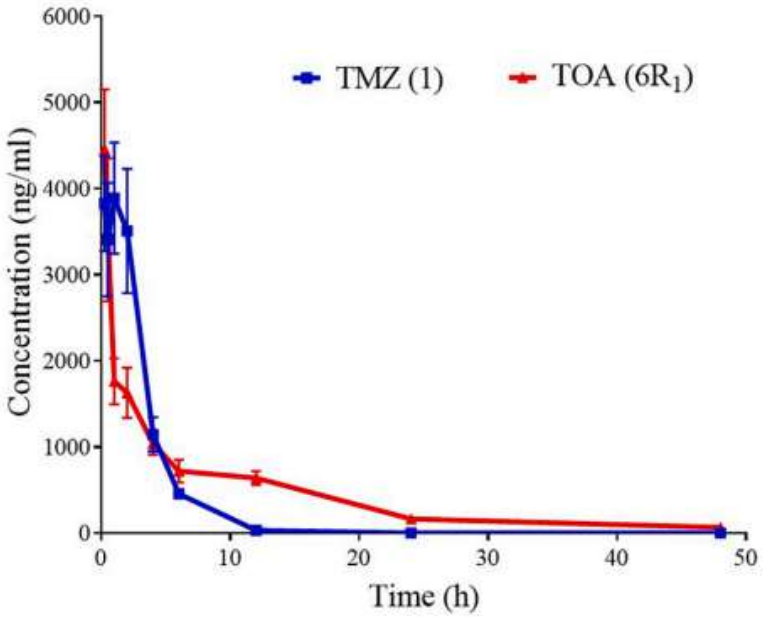

Figure 12. Pharmacokinetic studies of free TMZ and TOA (6R1) conjugate after intravenous (i.v.) administration in glioma-bearing SD rats. Each point represents a mean (n = 04) at a dose ~25 mg/kg.

6.8. Pharmacokinetic study

The plasma concentration profile of the samples is shown in Fig. 12, and different PK parameters are shown in Table 1 wherein there was an improvement in the pharmacokinetic profile of the TOA ($6R_1$) compared to free TMZ. Interestingly, there was a 7.7-fold increase in the half-life of TOA ($6R_1$) with respect to the TMZ, which has a half-life of 1.5 h. Similarly, the observed mean

residence time (MRT) of TOA ($6R_1$) was found to be increased ~3.8-fold in comparison to free TMZ, which has an MRT of 2.59 h.

Table:1 The non-compartmental pharmacokinetic parameters for TMZ and TOA in SD rat plasma (n=04) after i.v. bolus at a dose of 25 mg/kg.

Parameters	TMZ	TOA
C_{max} (ng/mL)	4298.506	5634.895
$t_{1/2}$ (h)	1.531	11.81
$AUC_{0\text{-last}}$ (ng.h/mL)	15441.3	21360.32
$AUC_{0\text{-}\infty}$ (ng.h/mL)	15445.11	22501.43
$AUMC_{0\text{-last}}$ (ng.h/mL)	40054.76	211031.1
$AUMC_{0\text{-}\infty}$ (ng.h/mL)	40246.14	285254.2
MRT (h)	2.59	9.87
V_z (mL/kg)	1430.12	7574.84
CL (mL/h/kg)	647.45	444.41

6.9. Efficacy study

C_6 cells-induced orthotopic glioma model in Sprague Dawley rats was used to evaluate the in vivo efficacy of synthesized TOA ($6R_1$) conjugate. The treatment was carried out for 80 days and as per the Kaplan Meier survival rate analysis (Fig. 13a), the animals in the positive control group died within 18 days, while in the TMZ (1) treated group, the survival rate was 40% after 80 days. Interestingly, a 100% of survival rate was observed in TOA ($6R_1$) treated group and the overall health was also found to be good. After C_6 cells injection, a sudden weight loss was observed in all the animals but once the treatment started the animals showed recovery in their overall weight (g). As shown in Fig. 13b, the positive control group animals showed continuous weight loss, while TMZ (1) and TOA ($6R_1$) treated animals showed better recovery. The morphological images of the brain of different groups of animals are shown in Fig. 13c. In the positive control group, animals tumor growth was observed at the injection site, while a significantly less affected area was observed in TMZ (1) and TOA ($6R_1$) treated groups. To confirm the physical tumor, the right/left hemisphere width (mm) ratio (Fig. 13d) and total brain weight (Fig. 13e) were examined.

As per the observation, the ratio of right/left hemisphere width was found to increase in the positive control animals w.r.t the normal control group. Interestingly, the ratio of right/left hemisphere width in the animals treated with TOA ($6R_1$) was significantly lesser than in the TMZ (1) treated group. A similar kind of result was observed when the total brain weight (g) was measured. The weight of the brain in the positive control group was significantly higher than that of the negative control group, while after treatment with TMZ (1) and TOA ($6R_1$) the brain weight (g) was significantly decreased as compared to positive control group. H&E staining was carried out for histological evaluation at the injection site. Fig. 14a shows the H&E-stained whole brain sections at higher magnification, the right lobe (C_6 cells injected) shows the tumor growth (red outline) while the left lobe (un-injected) shows normal vasculature. Overall, after treatment with TMZ (1) and TOA ($6R_1$), the tumor volume got reduced as compared to the positive control group. The TOA ($6R_1$), on the other hand, was more effective than TMZ (1) alone. The same can be seen in the high-resolution images of the tumor area obtained using a bright field inverted light microscope Fig. 14b. It has been reported that metastasis can be seen and to evaluate the same, the lungs of the animals were isolated after the completion of the study and fixed in Bouin's solution to see the metastatic nodules. As shown in Fig. 14c, the metastatic nodules were observed in positive control animals, but the number of nodules in TMZ (1) and TOA ($6R_1$) treated animals were significantly lower.

8. Statistical analysis

All of the data are shown as the mean ± standard deviation or standard error of the mean. Analysis of variance (ANOVA) followed by Tukey's multiple comparison test was used to compare the differences between the groups, and (*$P \leq 0.05$, ***$P \leq 0.01$, ***$P \leq 0.005$, and ****$P \leq 0.001$) was considered statistically significant.

4. Discussion

GBM has been considered as the most aggressive brain tumor [29], with TMZ as the first line treatment given orally as well as via the parenteral route [30]. Although TMZ is a potent molecule, it suffers from limitations including a short half-life [31], rapid metabolism [32], lesser accumulation in brain tissues (~1%) [13], and development of chemoresistance caused by overexpression of MGMT [33]. In the past few years, efforts have been made to improve its

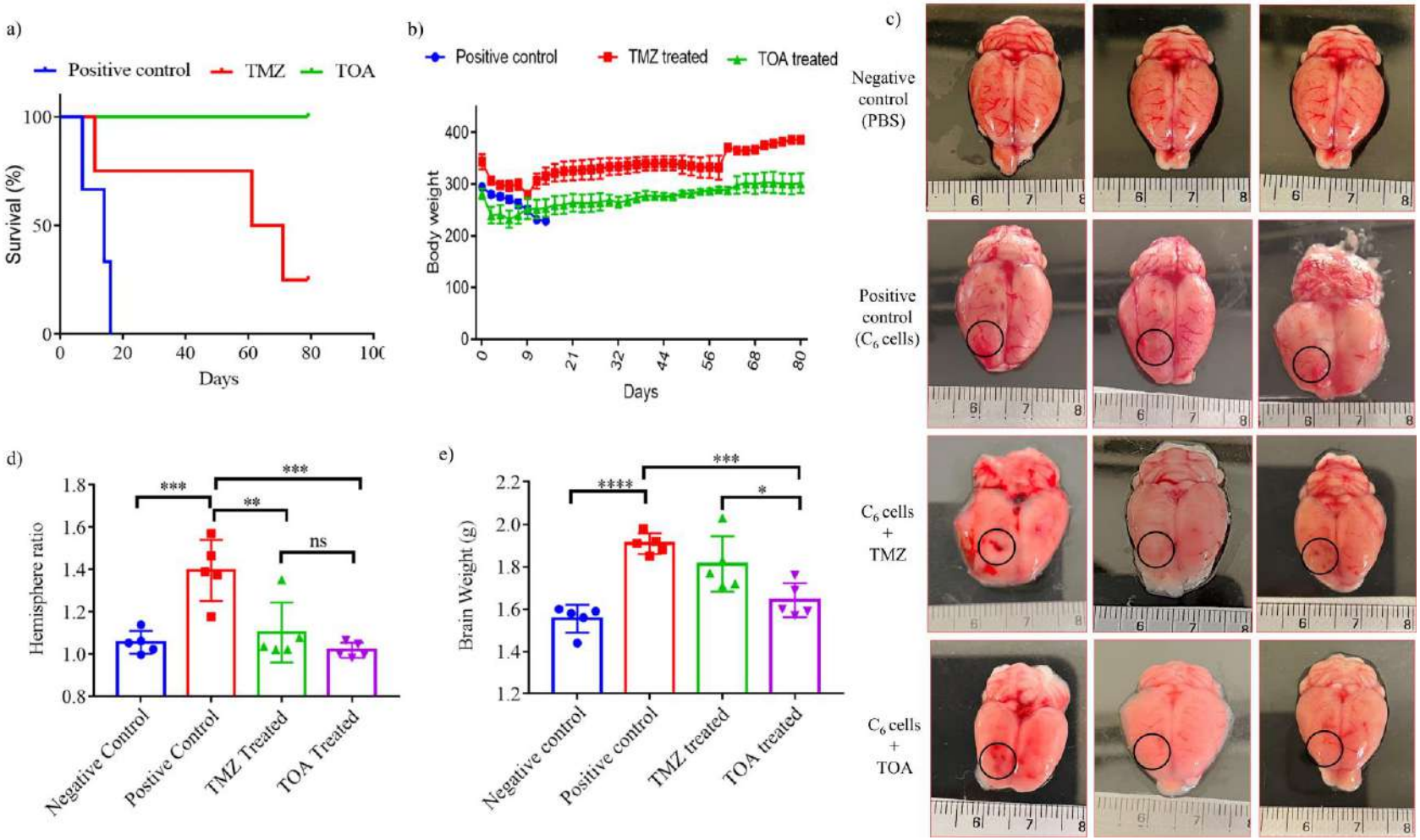

Figure 13. *In vivo* efficacy study of TOA (**6R$_1$**) conjugate and free TMZ **(1)** in C_6 cell induced orthotropic glioma bearing SD rats, a) Kaplan Meier survival rate, b) total body weight, c) whole brain images of animals from different treatment group, d) right/left hemisphere ratio and e) total brain weight.

efficiency utilizing nano carrier-based approaches, wherein some success has been seen. Among various strategies, hydrophobization of hydrophilic chemotherapeutic agents using a fatty acid is considered highly promising for enhancing their efficiency [22]. For instance, Li et al. showed that

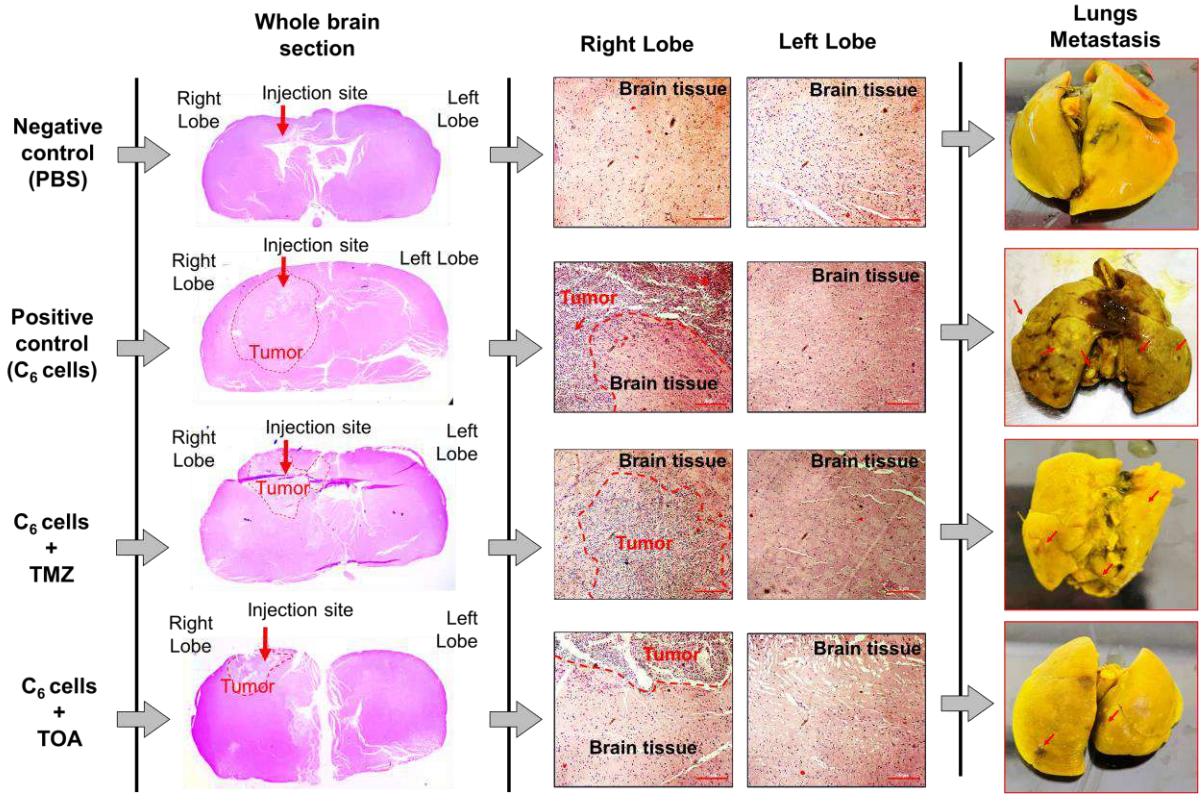

Figure 14. *In vivo* efficacy study of TOA **(6R$_1$)** conjugate and free TMZ **(1)** in C_6 cell induced orthotropic glioma bearing SD rats, a) H&E images of the whole brain sections, b) H&E images of the tumor around the injection site (right lobe (C_6 cells injected) and left lobe (non-injected)) and c) bouin's solution-stained lungs images.

the lipophilicity of doxorubicin was enhanced following conjugation with palmitic acid to create a prodrug with a pH-sensitive hydrazone linkage. Further, the prodrug was feasible to load into the hydrophobic core of polymeric micelles with a loading efficiency of 99.3 ± 5.7% [34]. We have earlier reported that conjugating lisofylline with linoleic acid increased its overall efficacy in treating diabetes with over a five-fold increase in half-life [22]. Due to hydrophobization, lisofylline-linoleic acid conjugate showed 75 ± 4.12% encapsulation efficiency with a practical drug loading of 9.29 ± 1.16% in mPEG-Poly-(carbonate-co-lactide) [mPEG-bP(CB-co-LA)] polymer [35]. Interestingly, fatty acids have also been explored for their anti-cancer activity in different types of cancers [36]. In 2017, Jiang et al. reported that oleic acid causes apoptosis in the

TSCC cell line and effectively kills cancer cells via autophagy [36]. In the current study, we have conjugated TMZ with fatty acids to obtain three different conjugates i.e. TOA ($6R_1$), TLA ($6R_2$), and TPA ($6R_3$). For conjugation, the TMZ was first converted into an acid derivative i.e. TMZ-acid (2), and characterized using FTIR, 1 H NMR, and mass spectrometry. Our results were in line with the previously reported synthesis of TMZ-acid [19]. The free -COOH group of fatty acids ($3R_{1–3}$) was modified to -CO-$NHNH_2$ (hydrazide derivative, $5R_{1–3}$) using a two-step reaction. The EDC/ HoBt amide coupling under cold conditions has been reported for good yield and purity, and therefore used for conjugation [37]. However, the major concern during the synthesis experiments was related to the stability of the TMZ, since it is prone to hydrolysis at physiological pH. Therefore, the purified TMZ-fatty acid conjugates ($6R_{1–3}$) were evaluated for the protons of -CH_3 at 3rd carbon by integrating the -CH_3 (3H) protons peak at δ 4.1 (a, -CH_3, s, 3H) in the 1 H NMR spectra. The integration was further confirmed with the 1 H proton at 6th carbon at δ 8.5 (b, -CH, s, 1H). The protons at both the carbons were found intact and therefore confirmed the intact form of TMZ in the final conjugate. The TMZ-fatty acid conjugates ($6R_{1–3}$) showed a purity of >98% with an overall yield of >50%. To evaluate the potency of the conjugates, we performed a cell viability assay, wherein the conjugates showed a ~5-fold decrease in the IC_{50} value indicating a synergistic anticancer effect with fatty acids. These findings were consistent with the published literature, where fatty acids including oleic acid, palmitic acid, and linoleic acid have shown anticancer activity [36,38,39]. Autophagy is a cellular process that could lead to apoptosis and oleic acid has been reported to induce autophagy in cancer cells [36]. Since, TMZ is also an autophagy inducer, therefore fatty acid has enhanced the overall anticancer effect of TMZ. Zhu et al. have earlier reported the antiproliferation effect of the palmitic acid in PC3 and DU145 prostate cancer cell lines with IC_{50} values of 10.72 μM and 16.83 μM, respectively [38]. Similarly, Jiang et al. also showed OA significantly inhibited cell growth in a dose and time-dependent manner with the IC_{50} values of 291 μM and 159 μM in CAL27 and UM1 cells, respectively after 24 h of incubation. Furthermore, the IC_{50} value was reduced to 228 μM and 78 μM in CAL27 and UM1 cells, respectively after 96 h of incubation. Overall, they concluded that OA could be used as a potent anticancer molecule by inducing apoptosis and autophagy by blocking the Akt/mTOR pathway [36]. Further, the cells treated with conjugates showed apoptosis and minimal necrosis as shown in Fig. 10. However, the major problem with glioma treatment using TMZ is resistance via MGMT upregulation. Kitenge et al. showed that the effect of TMZ in glioblastoma xenograft cells

in vivo (GBM43 and GBM44) was not significant due to modulation in the MGMT expression [40]. Since we got a potent cytotoxic effect of TMZ when conjugated with a fatty acid, it needs to be explored more to understand the effect of conjugates on MGMT expression. Fatty acids have been previously reported for their effect on MGMT depletion. In western blotting data, we observed that the MGMT expression was increased when cells were treated with TMZ alone, while the expression was decreased when cells were treated with the conjugates. This confirmed that the fatty acid plays a significant role in MGMT depletion and therefore makes TMZ more potent, sensitive, and effective in killing C_6 and U87-MG cells. This could also be attributed to the lower IC_{50} value in cells treated with TMZ fatty acid conjugates ($6R_{1–3}$) [41]. It has also been reported previously that combination therapy sensitized the glioma cells toward TMZ. In 2011, Wang et al. reported the effect of docosahexaenoic acid (DHA) on the sensitization of brain tumor cells toward etoposide therapy. Additionally, the reported reason was the synergistic effect of DHA by suppressing DNA repair genes [42]. Collectively, the outcomes of the in vitro studies concluded that the fatty acid conjugates of TMZ are more effective. At physiological pH, the TMZ undergoes hydrolysis, by means of decarboxylation at the C4 position of the six-membered ring, which results in the formation of MTIC and later forms AIC and a methyl diazonium ion. The effect of fatty acid conjugation on the degradation pattern of TMZ was examined using plasma stability studies, as shown in Fig. 11, the degradation of TMZ gets slowed down after conjugation and is dependent upon the degree of unsaturation of the fatty acid and maximum stability was observed in case of PA. Moreover, the unsaturation of fatty acid also contributes to the hydrophobicity of the final conjugate (Fig. 11), which could also be another reason for the sustained hydrolysis. Similar results were reported earlier by Singh et al., where the stability and efficiency of lysofylline depended upon the degree of unsaturation [43]. Moreover, the TOA ($6R_1$) conjugate was chosen further for in vivo studies since it has shown better in vitro apoptosis as compared to other conjugates. Also, as per the MTT assay, the free palmitic acid has a cell viability of 37% at 250 μM concentration, while oleic acid has a cell viability of 79% at the same concentration which indicated that free palmitic acid could be cytotoxic. Moreover, Oleic acid conjugate is more stable in plasma than linoleic acid conjugate. A C_6 cells-based orthotropic glioma model was developed in SD rats as reported previously [28]. Due to the complex anatomical location of the brain, it is challenging to observe the growth of the brain tumor physically. However, as per the reported literature, some parameters could be observed to predict the onset of tumor growth. For example, the number of

cells injected was kept constant i.e., 2×10^6 of C_6 cells, loss in body weight [44], right eye bulging, and reduced locomotion activity of the rat. The animals showing the above parameters were taken further and randomly divided into different groups. A pharmacokinetic study revealed the improved kinetic of fatty acid conjugate and the reason might be the improvement in the stability of the conjugate at the physiological pH of the blood after conjugation to a fatty acid. A similar observation has been reported by Jin et al. for prodrugs of gemcitabine prepared by conjugating it with lipid derivatives. As per their observations, the PK parameters of gemcitabine get improved after conjugation with the lipids [45]. Similar reports were by Italia et al., wherein the conjugation of lysofylline with a lipid improved its in vivo stability and PK profile. More specifically, the LSF-LA prodrug exhibited reduced protein binding and showed a significantly higher half-life (5.7-fold), and higher apparent volume of distribution (5.3-fold) than free LSF [22].The TOA ($6R_1$) conjugate showed better outcomes in terms of overall survival rate, brain weight, hemisphere width, and reduction in tumor volume, which could be attributed to the improved efficacy after fatty acid conjugation. Similar observations were reported by Yu et al., where a series of temozolomide ester (TMZEs) prodrugs were synthesized, having different chain lengths, which lead to an increase in lipophilicity due to the esterification of the TMZ. The TMZEs showed stability in plasma and brain homogenates showed better cell uptake and cytotoxicity in the C_6 cell line at the lower dose, and showed ~2-fold improvement in survival rate [46]. Interestingly, the study demonstrated that the physicochemical and biological properties of TMZ get improved after esterification, which further increases lipophilicity, membrane absorption, and therapeutic effect [46]. In order to understand the metastasis, the lungs were stained with Bouin's solution. A higher number of metastatic nodules were present in the positive control group, while there was a reduction in the metastatic nodules in TMZ and TOA-treated animals. Collectively, the TOA conjugate is a better therapeutic option for the treatment of glioma, and further studies as warranted for its development.

9. Impact of the research in the advancement of knowledge or benefit to mankind

Glioblastoma multiform is the deadliest brain tumor with a median survival rate of less than 15 months. Temozolomide is the standard chemotherapeutic agent available in the market as a tablet and capsule form and shows 100% bioavailability. Despite its ability to cross the blood-brain barrier, the TMZ possesses various limitations that compromise its therapeutic efficiency, these limitations include short half-life (1.5 h), rapid metabolism, lesser accumulation at the tumor site, lower brain bioavailability, resistance due to MGMT, and systemic toxicity. Such limitations make temozolomide ineffective for the treatment of gliomas and the reported survival rate with temozolomide therapy (<5%) consolidates the persistence. Ample strategies have been adopted for improving the therapeutic efficacy of TMZ, The most recent example is the use of a nanocarrier system to improve the circulation half-life and brain tumor accumulation, however, due to the amphiphilic nature of TMZ it is challenging to load the TMZ in the hydrophobic core of the nanocarriers. In current research work, we synthesized novel fatty acid conjugates of TMZ to improve the hydrophobicity and therapeutic efficacy. The TMZ fatty acids were found more potent, improved pharmacokinetic behavior, and were less prone to resistance. Moreover, the TMZ-fatty acid was hydrophobic in nature and could be loaded in the nanocarrier system for brain tumor-specific delivery. Overall, the novel TMZ-fatty acid conjugates have all the translational properties and could be explored to fulfill the unmet need for chemotherapy for brain cancer.

10. Literature references

[1] K. Rock, O. McArdle, P. Forde, M. Dunne, D. Fitzpatrick, B. O'Neill, C. Faul, A clinical review of treatment outcomes in glioblastoma multiforme--the validation in a non-trial population of the results of a randomised Phase III clinical trial: has a more radical approach improved survival?, The British journal of radiology, 85 (2012) e729-733.

[2] J.P. Thakkar, T.A. Dolecek, C. Horbinski, Q.T. Ostrom, D.D. Lightner, J.S. Barnholtz-Sloan, J.L. Villano, Epidemiologic and molecular prognostic review of glioblastoma, Cancer Epidemiol Biomarkers Prev, 23 (2014) 1985-1996.

[3] D.N. Louis, H. Ohgaki, O.D. Wiestler, W.K. Cavenee, P.C. Burger, A. Jouvet, B.W. Scheithauer, P. Kleihues, The 2007 WHO classification of tumours of the central nervous system, Acta neuropathologica, 114 (2007) 97-109.

[4] M. Robert, M. Wastie, Glioblastoma multiforme: a rare manifestation of extensive liver and bone metastases, Biomedical imaging and intervention journal, 4 (2008) e3.

[5] O.G. Taylor, J.S. Brzozowski, K.A. Skelding, Glioblastoma Multiforme: An Overview of Emerging Therapeutic Targets, Frontiers in oncology, 9 (2019) 963.

[6] J. Lee, K. Kay, K. Troike, M.S. Ahluwalia, J.D. Lathia, Sex Differences in Glioblastoma Immunotherapy Response, Neuromolecular medicine, 24 (2022) 50-55.

[7] S.Y. Lee, Temozolomide resistance in glioblastoma multiforme, Genes & diseases, 3 (2016) 198-210.

[8] H. Strobel, T. Baisch, R. Fitzel, K. Schilberg, M.D. Siegelin, G. Karpel-Massler, K.M. Debatin, M.A. Westhoff, Temozolomide and Other Alkylating Agents in Glioblastoma Therapy, Biomedicines, 7 (2019).

[9] M. Rubio-Camacho, J.A. Encinar, M.J. Martínez-Tomé, R. Esquembre, C.R. Mateo, The Interaction of Temozolomide with Blood Components Suggests the Potential Use of Human Serum Albumin as a Biomimetic Carrier for the Drug, Biomolecules, 10 (2020).

[10] H.S. Friedman, T. Kerby, H. Calvert, Temozolomide and treatment of malignant glioma, Clinical cancer research : an official journal of the American Association for Cancer Research, 6 (2000) 2585-2597.

[11] M.A. Taylor, B.C. Das, S.K. Ray, Targeting autophagy for combating chemoresistance and radioresistance in glioblastoma, Apoptosis : an international journal on programmed cell death, 23 (2018) 563-575.

[12] M. Fresnais, S. Turcan, D. Theile, J. Ungermann, Y. Abou Zeed, J.R. Lindner, M. Breitkopf, J. Burhenne, W.E. Haefeli, R. Longuespée, Approaching Sites of Action of Temozolomide for Pharmacological and Clinical Studies in Glioblastoma, Biomedicines, 10 (2021).

[13] K. Bouzinab, H. Summers, J. Zhang, M.F.G. Stevens, C.J. Moody, L. Turyanska, N.R. Thomas, P. Gershkovich, M.B. Ashford, E. Vitterso, L.C.D. Storer, R. Grundy, T.D. Bradshaw, In search of effective therapies to overcome resistance to Temozolomide in brain tumours, Cancer drug resistance (Alhambra, Calif.), 2 (2019) 1018-1031.

[14] R. Jatyan, P. Singh, D.K. Sahel, Y.G. Karthik, A. Mittal, D. Chitkara, Polymeric and small molecule-conjugates of temozolomide as improved therapeutic agents for glioblastoma multiforme, Journal of controlled release : official journal of the Controlled Release Society, 350 (2022) 494-513.

[15] J. Gao, Z. Wang, H. Liu, L. Wang, G. Huang, Liposome encapsulated of temozolomide for the treatment of glioma tumor: preparation, characterization and evaluation, Drug discoveries & therapeutics, 9 (2015) 205-212.

[16] X. Song, L. Xie, M. Chang, X. Geng, X. Wang, T.C. Chen, X. Song, Temozolomide-perillyl alcohol conjugate downregulates O(6)-methylguanin DNA methltransferase via inducing ubiquitination-dependent proteolysis in non-small cell lung cancer, Cell death & disease, 9 (2018) 202.

[17] L. Xie, X. Song, W. Guo, X. Wang, L. Wei, Y. Li, L. Lv, W. Wang, T.C. Chen, X. Song, Therapeutic effect of TMZ-POH on human nasopharyngeal carcinoma depends on reactive oxygen species accumulation, Oncotarget, 7 (2016) 1651-1662.
[18] S.M. Ward, M. Skinner, B. Saha, T. Emrick, Polymer-Temozolomide Conjugates as Therapeutics for Treating Glioblastoma, Molecular pharmaceutics, 15 (2018) 5263-5276.
[19] K. Du, Q. Xia, H. Heng, F. Feng, Temozolomide-Doxorubicin Conjugate as a Double Intercalating Agent and Delivery by Apoferritin for Glioblastoma Chemotherapy, ACS applied materials & interfaces, 12 (2020) 34599-34609.
[20] Y. Peng, J. Huang, H. Xiao, T. Wu, X. Shuai, Codelivery of temozolomide and siRNA with polymeric nanocarrier for effective glioma treatment, International journal of nanomedicine, 13 (2018) 3467-3480.
[21] M. Bhat, R. Jatyan, A. Mittal, R.I. Mahato, D. Chitkara, Opportunities and challenges of fatty acid conjugated therapeutics, Chemistry and physics of lipids, 236 (2021) 105053.
[22] K.S. Italiya, S. Mazumdar, S. Sharma, D. Chitkara, R.I. Mahato, A. Mittal, Self-assembling lisofylline-fatty acid conjugate for effective treatment of diabetes mellitus, Nanomedicine : nanotechnology, biology, and medicine, 15 (2019) 175-187.
[23] X.Y. Ke, B.J. Zhao, X. Zhao, Y. Wang, Y. Huang, X.M. Chen, B.X. Zhao, S.S. Zhao, X. Zhang, Q. Zhang, The therapeutic efficacy of conjugated linoleic acid - paclitaxel on glioma in the rat, Biomaterials, 31 (2010) 5855-5864.
[24] A. Göder, G. Nagel, A. Kraus, B. Dörsam, N. Seiwert, B. Kaina, J. Fahrer, Lipoic acid inhibits the DNA repair protein O 6-methylguanine-DNA methyltransferase (MGMT) and triggers its depletion in colorectal cancer cells with concomitant autophagy induction, Carcinogenesis, 36 (2015) 817-831.
[25] D.K. Sahel, M. Salman, M. Azhar, S.G. Goswami, V. Singh, M. Dalela, S. Mohanty, A. Mittal, S. Ramalingam, D. Chitkara, Cationic lipopolymeric nanoplexes containing the CRISPR/Cas9 ribonucleoprotein for genome surgery, Journal of materials chemistry. B, 10 (2022) 7634-7649.
[26] S. Sharma, S.S. Pukale, D.K. Sahel, D.S. Agarwal, M. Dalela, S. Mohanty, R. Sakhuja, A. Mittal, D. Chitkara, Folate-Targeted Cholesterol-Grafted Lipo-Polymeric Nanoparticles for Chemotherapeutic Agent Delivery, AAPS PharmSciTech, 21 (2020) 280.
[27] N. Clemente, B. Ferrara, C.L. Gigliotti, E. Boggio, M.T. Capucchio, E. Biasibetti, D. Schiffer, M. Mellai, L. Annovazzi, L. Cangemi, E. Muntoni, G. Miglio, U. Dianzani, L. Battaglia, C. Dianzani, Solid Lipid Nanoparticles Carrying Temozolomide for Melanoma Treatment. Preliminary In Vitro and In Vivo Studies, International journal of molecular sciences, 19 (2018).
[28] G. Tianqin, C. Chunlei, W. Jingjing, Synergistic Anti-glioma Effects in Vitro and in Vivo of Enediyne Antibiotic Neocarzinostatin and Paclitaxel via Enhanced Growth Delay and Apoptosis-Induction, Biological & pharmaceutical bulletin, 39 (2016) 1623-1630.
[29] D.J. Lundy, K.J. Lee, I.C. Peng, C.H. Hsu, J.H. Lin, K.H. Chen, Y.W. Tien, P.C.H. Hsieh, Inducing a Transient Increase in Blood-Brain Barrier Permeability for Improved Liposomal Drug Therapy of Glioblastoma Multiforme, ACS nano, 13 (2019) 97-113.
[30] S. Chibbaro, L. Benvenuti, A. Caprio, S. Carnesecchi, F. Pulerà, F. Faggionato, D. Serino, C. Galli, M. Andreuccetti, N. Buxton, R. Gagliardi, Temozolomide as first-line agent in treating high-grade gliomas: phase II study, Journal of neuro-oncology, 67 (2004) 77-81.
[31] H. Zhang, S. Gao, Temozolomide/PLGA microparticles and antitumor activity against glioma C6 cancer cells in vitro, International journal of pharmaceutics, 329 (2007) 122-128.
[32] S.D. Baker, M. Wirth, P. Statkevich, P. Reidenberg, K. Alton, S.E. Sartorius, M. Dugan, D. Cutler, V. Batra, L.B. Grochow, R.C. Donehower, E.K. Rowinsky, Absorption, metabolism, and excretion of 14C-temozolomide following oral administration to patients with advanced cancer, Clinical cancer research : an official journal of the American Association for Cancer Research, 5 (1999) 309-317.
[33] C. Fang, K. Wang, Z.R. Stephen, Q. Mu, F.M. Kievit, D.T. Chiu, O.W. Press, M. Zhang, Temozolomide nanoparticles for targeted glioblastoma therapy, ACS applied materials & interfaces, 7 (2015) 6674-6682.

[34] F. Li, C. Snow-Davis, C. Du, M.L. Bondarev, M.D. Saulsbury, S.O. Heyliger, Preparation and Characterization of Lipophilic Doxorubicin Pro-drug Micelles, Journal of visualized experiments : JoVE, (2016).
[35] K.S. Italiya, M. Basak, S. Mazumdar, D.K. Sahel, R. Shrivastava, D. Chitkara, A. Mittal, Scalable Self-Assembling Micellar System for Enhanced Oral Bioavailability and Efficacy of Lisofylline for Treatment of Type-I Diabetes, Molecular pharmaceutics, 16 (2019) 4954-4967.
[36] L. Jiang, W. Wang, Q. He, Y. Wu, Z. Lu, J. Sun, Z. Liu, Y. Shao, A. Wang, Oleic acid induces apoptosis and autophagy in the treatment of Tongue Squamous cell carcinomas, Sci Rep, 7 (2017) 11277.
[37] S. Sharma, S. Mazumdar, K.S. Italiya, T. Date, R.I. Mahato, A. Mittal, D. Chitkara, Cholesterol and Morpholine Grafted Cationic Amphiphilic Copolymers for miRNA-34a Delivery, Molecular pharmaceutics, 15 (2018) 2391-2402.
[38] S. Zhu, W. Jiao, Y. Xu, L. Hou, H. Li, J. Shao, X. Zhang, R. Wang, D. Kong, Palmitic acid inhibits prostate cancer cell proliferation and metastasis by suppressing the PI3K/Akt pathway, Life sciences, 286 (2021) 120046.
[39] X. Lu, H. Yu, Q. Ma, S. Shen, U.N. Das, Linoleic acid suppresses colorectal cancer cell growth by inducing oxidant stress and mitochondrial dysfunction, Lipids in health and disease, 9 (2010) 106.
[40] G.J. Kitange, B.L. Carlson, M.A. Schroeder, P.T. Grogan, J.D. Lamont, P.A. Decker, W. Wu, C.D. James, J.N. Sarkaria, Induction of MGMT expression is associated with temozolomide resistance in glioblastoma xenografts, Neuro-oncology, 11 (2009) 281-291.
[41] L. Persano, F. Pistollato, E. Rampazzo, A. Della Puppa, S. Abbadi, C. Frasson, F. Volpin, S. Indraccolo, R. Scienza, G. Basso, BMP2 sensitizes glioblastoma stem-like cells to Temozolomide by affecting HIF-1α stability and MGMT expression, Cell death & disease, 3 (2012) e412.
[42] F. Wang, K. Bhat, M. Doucette, S. Zhou, Y. Gu, B. Law, X. Liu, E.T. Wong, J.X. Kang, T.C. Hsieh, S.Y. Qian, E. Wu, Docosahexaenoic acid (DHA) sensitizes brain tumor cells to etoposide-induced apoptosis, Current molecular medicine, 11 (2011) 503-511.
[43] A.K. Singh, K.S. Italiya, S. Narisepalli, D. Chitkara, A. Mittal, Role of Chain Length and Degree of Unsaturation of Fatty Acids in the Physicochemical and Pharmacological Behavior of Drug-Fatty Acid Conjugates in Diabetes, Journal of medicinal chemistry, 64 (2021) 14217-14229.
[44] E.S. Redgate, M. Deutsch, S.S. Boggs, Time of death of CNS tumor-bearing rats can be reliably predicted by body weight-loss patterns, Laboratory animal science, 41 (1991) 269-273.
[45] Y. Jin, Y. Lian, L. Du, S. Wang, C. Su, C. Gao, Self-assembled drug delivery systems. Part 6: in vitro/in vivo studies of anticancer N-octadecanoyl gemcitabine nanoassemblies, Int J Pharm, 430 (2012) 276-281.
[46] Y. Yu, L. Wang, J. Han, A. Wang, L. Chu, X. Xi, R. Kan, C. Sha, K. Sun, Synthesis and Characterization of a Series of Temozolomide Esters and Its Anti-glioma Study, Journal of pharmaceutical sciences, 110 (2021) 3431-3438.

Declaration

The aforementioned research work is performed by me as a part of my Ph.D. thesis. Some part of these findings has been published, while the rest are under compilation and preparation for submission.

(Ph.D. Research Scholar)

BITS-Pilani, Pilani Campus

333031, Pilani, India